

MASERS AND BROAD-LINE MAPPING FAVOR MAGNETICALLY-DOMINATED AGN ACCRETION DISKS

PHILIP F. HOPKINS^{1,*}, DALYA BARON², AND JOANNA M. PIOTROWSKA¹

¹TAPIR, Mailcode 350-17, California Institute of Technology, Pasadena, CA 91125, USA and

²Kavli Institute for Particle Astrophysics & Cosmology, Stanford University, CA 94305, USA

Version January 13, 2026

ABSTRACT

We present a novel and powerful constraint on the physics of supermassive black hole (BH) accretion disks. We show that in the outer disk (radii $R \gtrsim 0.01$ pc or $\gtrsim 1000 R_G$), models supported by thermal or radiation pressure predict disk masses which are much larger than the BH mass and increase with radius – i.e. rapidly-rising, extremely non-Keplerian rotation curves. More generally, we show that any observational upper limit to the deviation from Keplerian potentials at these radii directly constrains the physical form of the pressure in disks. We then show that existing maser and broad line region (BLR) kinematic observations immediately rule out the classic thermal-pressure-dominated Shakura Sunyaev-like α -disk model, and indeed rule out any thermal or radiation (or cosmic-ray) pressure-dominated disk, as the required temperatures and luminosities of the gas at large radii would exceed those observed by orders of magnitude. We show that models where the pressure comes entirely from turbulence (without thermal, radiation, or magnetic sources) could in principle be viable but would require turbulent Toomre $Q \gtrsim 100$, far larger than predicted by self gravitating/gravito-turbulent models. However, recently proposed models of magnetic pressure-dominated disks agree with all of the observational constraints. These magnetically-dominated models also appear to agree better with constraints on maser magnetic fields, compared to the other possibilities. Observations appear to strongly favor the hypothesis that the outer regions of BH accretion disks are in the “hyper-magnetized” state.

Subject headings: accretion, accretion disks — black holes — active galactic nuclei, quasars — masers, emission lines — magnetic fields, radiation

1. INTRODUCTION

Quasars and active galactic nuclei (AGN) are powered by accretion disks around supermassive BHs (Schmidt 1963; Soltan 1982). The overwhelming majority of accretion disk models assume that the accretion disk itself is thermal and/or radiation-pressure dominated, and so is qualitatively similar to the classic Shakura & Sunyaev (1973); Novikov & Thorne (1973)-like (SS73) α disk model. This includes many variant disk models including thin or “slim,” magnetically elevated, and advection-dominated (Frank et al. 2002; Abramowicz & Fragile 2013). Recently, however, simulations following magnetized gas inflows self-consistently from star-forming ISM through accretion-disk scales in Hopkins et al. (2024a,b,d) found a qualitatively different type of accretion disk emerges: so-called “hyper-magnetized” or “flux-frozen” disks, whose midplane pressure is dominated by toroidal magnetic fields amplified and stretched from ISM fields. This has now been seen in other simulation contexts including lower-accretion rate elliptical galaxies (Guo et al. 2024); intermediate-mass to $\sim 10^6 M_\odot$ BHs in dense star clusters resembling “little red dots” (Shi et al. 2024a,b); some magnetized first-stars simulations (Luo & Shlosman 2024); circum-binary magnetized cloud collapse (Wang et al. 2025); followups to smaller (near-horizon) radii (Kaaz et al. 2025; Hopkins et al. 2025); as well as older simulations of more idealized setups (Gaburov et al. 2012) and similar recent studies (Squire et al. 2025; Guo et al. 2025). Analytic models (Hopkins et al. 2024c; Hopkins 2025) have argued that such disks should be ubiquitous around high-accretion rate SMBHs, and have properties unlike traditional α -disks.

One of the most dramatic differences between these hyper-magnetized/flux-frozen (plasma $\beta \equiv P_{\text{thermal}}/P_{\text{magnetic}} \ll 1$) and traditional ($\beta \gg 1$) α -disks is in the disk mass, especially

at large radii/distances from the BH. Because the Maxwell stresses are, by definition, strong in the hyper-magnetized disks, accretion is fundamentally dynamical, i.e. the inflow timescale ($t_{\text{acc}} \sim M_{\text{disk}}/\dot{M}$) at radii from the BH radius of influence (BHROI) to horizon scales is of order the orbital time ($t_{\text{acc}} \sim 10\Omega^{-1}$ in terms of the disk orbital frequency Ω). In contrast, in an α -disk, $t_{\text{acc}} \sim \alpha^{-1} (v_c/c_s)^2 \Omega^{-1} \sim 10^6 - 10^8 \Omega^{-1}$ in the outer disk ($\sim 0.01 - 10$ pc), i.e. accretion proceeds secularly over millions of orbits at large radii. A necessary consequence of this is that, in order to provide a given observed accretion rate and/or luminosity, the outer disk must be orders-of-magnitude more massive in α -disk models compared to hyper-magnetized disks. At radii $\gtrsim 0.01$ pc, this in turn leads to a major qualitative difference: α disks (whether thermal-or-radiation pressure dominated) are predicted to be much more massive than the BH itself ($M_{\text{disk}}(< R) \sim \pi \Sigma_{\text{gas}} R^2 \gg M_{\text{BH}}$), meaning that the gravitational potential becomes qualitatively modified and the rotation curve or circular velocity $V_c \equiv \sqrt{G M_{\text{total}}(< R)/R}$ goes from the standard declining Keplerian behavior ($V_c \propto R^{-1/2}$) to *rising* ($V_c \propto R^{3/8}$ or $R^{2/3}$, like in the central few kpc of galaxies). In contrast, hyper-magnetized disks have $M_{\text{disk}}(< R) \ll M_{\text{BH}}$ so the potential remains approximately Keplerian out to the BHROI $R_{\text{BHROI}} \equiv G M_{\text{BH}}/\sigma_{\text{gal}}^2 \sim 10$ pc ($M_{\text{BH}}/10^8 M_\odot$) ($\sigma_{\text{gal}}/200 \text{ km s}^{-1}$) $^{-2}$ (in terms of the galactic velocity dispersion σ_{gal}) exterior to which, by definition, the galactic potential of stars and dark matter dominate over the BH.

This range of radii falls well within the range where excellent constraints on the kinematics and rotation curves of gas around many AGN exist, from a combination of maser, infrared (dust) and optical (broad-line) interferometric, and reverberation-mapping constraints mapping out the dynamics of gas as a function of BH-centric radius R . In this manuscript, we show

*E-mail: phopkins@caltech.edu

that this leads to robust qualitative constraints on the form of the pressure supporting the accretion disk, and very clearly rules out thermal or radiation pressure-dominated accretion disks at $R \gtrsim 0.01$ pc around most accreting SMBHs. We show that, completely independent of detailed assumptions of the accretion disk model, *any* thermal or radiation or cosmic-ray pressure dominated accretion disk at these radii compatible with the observations of kinematics would grossly violate other fundamental observational constraints (e.g. predicting orders-of-magnitude larger luminosities than observed). We also show that many of these models appear to be in tension with upper limits on the magnetic field strengths observed at these radii. In contrast, we show that the existing predictions of simple analytic similarity models for flux-frozen, hypermagnetized disks appear to agree naturally with all of these observational constraints.

2. THEORETICAL BASIS

As emphasized in § 1, different families of accretion disk models result in different scalings of circular velocity with distance from the black hole (shown in Fig. 1). In what follows, we will consider different models for the accretion disk pressure (thermal, radiation, magnetic, turbulent, cosmic-ray) in turn. For each, we will present the “standard” literature model, using the specific scalings from canonical papers deriving models under the assumption that the given pressure is dominant in the midplane (summarized in Figs. 1-4). But we will then consider much more general constraints, asking “what if” we removed normal self-consistency assumptions and simply allowed that pressure (e.g. the thermal pressure or temperature) to have any value we wanted, in order to show that most models cannot possibly fit kinematic observations without severely violating other basic observational constraints. It is therefore helpful to define some basic background terms and scalings.

The defining assumption generic to accretion disk models is that some stress or torque removes angular momentum at a rate balancing the change in orbital angular momentum in the disk (e.g. Abramowicz & Fragile 2013). This can be written as $\dot{M} = 3\pi\nu_{\text{v, eff}}\Sigma_{\text{gas}}$ in terms of the accretion rate \dot{M} , disk surface density Σ_{gas} , and effective viscosity $\nu_{\text{v, eff}} \equiv \varpi_{\text{v}}\nu_e^2/\Omega \equiv \Pi/\Omega\rho$ where ρ is the midplane gas density, $\Omega \equiv V_{\text{c}}/R$ at some distance R in a potential with circular velocity $V_{\text{c}}^2 \equiv GM_{\text{enc}}(< R)/R$ (total enclosed mass $M_{\text{enc}}(< R)$ – note we do not assume a Keplerian potential) and either some effective transport (turbulent, Alfvén, or other) velocities ν_e or relevant component of the stress tensor Π driving accretion, with ϖ_{v} some order-unity prefactor that depends on details of e.g. the vertical disk profile.¹ Since the total disk mass enclosed is an increasing function of R , we can integrate over $2\pi R dR$ from $R = 0$ to R , and obtain:

$$M_{\text{gas}}(< R) \approx 3\varpi \left(\frac{\Pi_{\text{eff}}}{\rho} \right)^{-1} \dot{M} \Omega R^2. \quad (1)$$

Again, this is true by definition for any accretion disk model. Now, combining this with the definition of V_{c} and the Keplerian

¹ For our purposes these factors ϖ vary quite weakly – by tens of percents or so – compared to the orders-of-magnitude differences between different models for the disk pressure, so we can safely treat them as unity here.

velocity V_K (V_{c} if $M_{\text{enclosed}}(< R)$ were equal to M_{BH}):

$$V_{\text{c}} \equiv \sqrt{\frac{GM_{\text{enclosed}}(< R)}{R}}, \quad (2)$$

$$V_K \equiv \sqrt{\frac{GM_{\text{BH}}}{R}}, \quad (3)$$

we have

$$\frac{V_{\text{c}}^2}{V_K^2} \approx \frac{M_{\text{BH}} + M_{\text{gas}}(< R)}{M_{\text{BH}}} \approx 1 + \psi \left[\sqrt{1 + \frac{\psi^2}{4}} + \frac{\psi}{2} \right], \quad (4)$$

where the dimensionless quantity ψ is given by

$$\begin{aligned} \psi \equiv 3\varpi \left(\frac{\Pi_{\text{eff}}}{\rho} \right)^{-1} \frac{\dot{M}V_K R}{M_{\text{BH}}} &\sim \frac{3L}{\epsilon_r c^2} \left(\frac{\Pi_{\text{eff}}}{\rho} \right)^{-1} \sqrt{\frac{GR}{M_{\text{BH}}}} \\ &\sim \frac{3\dot{m}}{t_S} \left(\frac{\Pi_{\text{eff}}}{\rho} \right)^{-1} \sqrt{GM_{\text{BH}}R} \\ &\sim 4 \left(\frac{\Pi_{\text{eff}}}{\rho \text{ (km s}^{-1}\text{)}^2} \right)^{-1} \dot{m} m_7^{1/2} r_{0.1}^{1/2}. \end{aligned} \quad (5)$$

In the last equations we define some convenient units: $L = \epsilon_r \dot{M} c^2$, Salpeter time $t_S \approx 5 \times 10^7$ yr, $r_{0.1} \equiv R/0.1$ pc, $m_7 \equiv M_{\text{BH}}/10^7 M_{\odot}$, and $\dot{m} \equiv 0.1 \dot{M} c^2/L_{\text{Edd}}$ (i.e. accretion rate relative to Eddington for a radiative efficiency of $\epsilon_r \sim 0.1$).

Let us define the upper limit on the deviation of the circular velocity from Keplerian as:

$$V_{\text{c}}^2 \leq V_K^2 (1 + \Delta) \quad (6)$$

i.e. $(V_{\text{c}}^2 - V_K^2)/V_K^2 \leq \Delta$ (or equivalently if $V_{\text{c}}/V_K < 1 + \delta$, $\Delta = 2\delta + \delta^2$). This is equivalent to $\psi \leq \Delta/\sqrt{1 + \Delta}$, or

$$\frac{P_{\text{tot}}}{\rho} > \frac{\Pi_{\text{eff}}}{\rho} > \frac{3\dot{m}\sqrt{GM_{\text{BH}}R(1 + \Delta)}}{t_S \Delta}. \quad (7)$$

In other words, any observed upper limit to Δ , i.e. close-to-Keplerian behavior of the rotation curve, sets a *lower* limit to the ratio P_{tot}/ρ , i.e. the specific pressure-per-unit-mass, needed to explain the observed accretion rate or luminosity in *any* self-consistent accretion disk model. Conversely, a given accretion disk model, which assumes some source of pressure Π/ρ in the midplane, predicts a *lower* limit to Δ , i.e. a minimum mass of the accretion disk needed to power the observed accretion, and therefore a minimum deviation from Keplerian rotation (Fig. 1).

In the last equation, we have used the fact that in any reasonable model, $\Pi_{\text{eff}} < P_{\text{tot}}$ – i.e. the salient net stress component causing dissipation and angular momentum transfer cannot significantly exceed the total stress/pressure. At any given radius, we can simply define

$$\Pi_{\text{eff}} \equiv \alpha P_{\text{tot}} \lesssim P_{\text{tot}}, \quad (8)$$

(i.e. $\alpha \lesssim 1$). Note we define this parameter by analogy to the classic α -disk model, but those models specifically assume α is a constant (we allow it to be a function of radius or other properties) and that the pressure is primarily thermal. So we stress in our case that this is simply a convenient parameterization and there is no loss of generality.

Note that because $\Delta \ll 1$ for the cases of greatest interest, i.e. the potentials are not far from Keplerian, we can also use the above scalings with the fact that the scale height of the disk

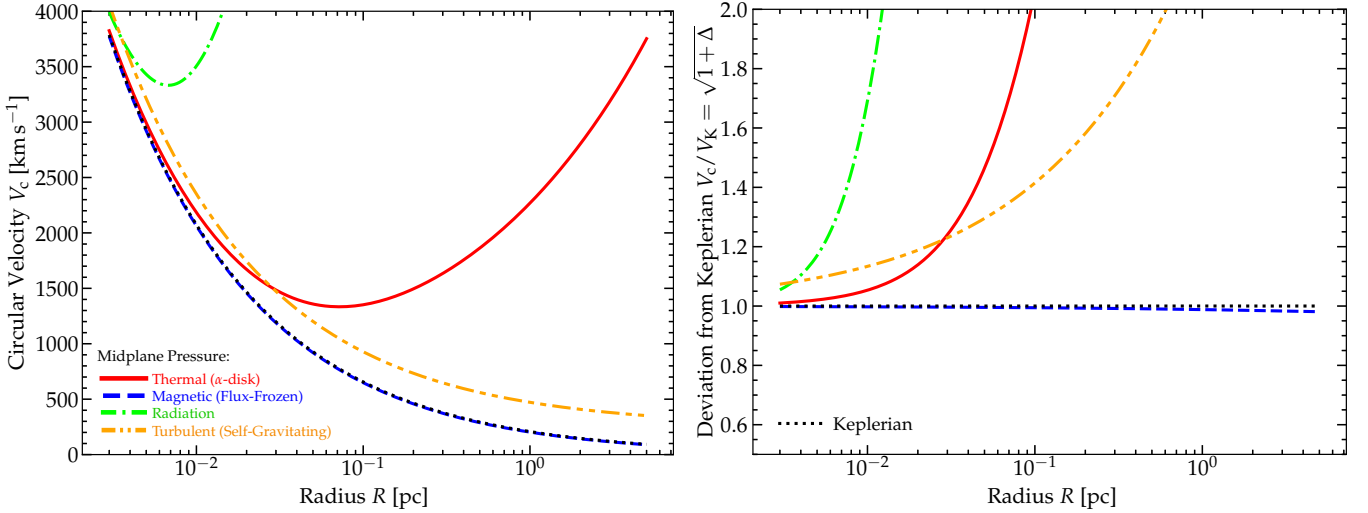


FIG. 1.— Expected scaling of gas circular velocity with radius and its deviation from Keplerian motion for different accretion disk models. Lines correspond to standard accretion disk models assuming a $M_{\text{BH}} = 10^7 M_{\odot}$ accreting near-Eddington ($m_7 = \dot{m} = 1$) with an effective accretion-stress-to-total-pressure ratio $\alpha = 0.1$. We assume the disk total pressure is primarily: (1) thermal (a standard SS73-like or α -disk; § 4.1); (2) magnetic (a flux-frozen or hyper-magnetized disk; § 4.2); (3) radiation (a slim or radiation-pressure-supported disk; § 4.3); (4) turbulent (constant- Q_0 or gravito-turbulent, with $Q_0 = 0.04$ as required to fit some NGC 1068 observations with this model; § 4.4). For each, we plot the predicted $V_c^2(R) \equiv GM_{\text{enc}}(< R)/R = G [M_{\text{BH}} + M_{\text{disk}}(< R)]/R$. We compare to Keplerian (in absolute units at *left* or relative *right*). Per § 2, different assumptions about what dominates the pressure in the outer disk, for a given BH mass and luminosity, give very different predictions for the disk mass, with larger disk masses producing large deviations from Keplerian circular velocity curves (even rapidly-rising curves). Attempting to “re-tune” the thermal or radiation models by arbitrarily changing the predicted temperatures or opacities to suppress the deviations from Keplerian lead to other, immediately ruled-out predictions (like ~ 10 orders of magnitude larger luminosities).

in a Keplerian potential $H/R \sim (\sqrt{P_{\text{tot}}/\rho})/v_K$ to turn Eq. 7 into a lower limit on H/R :

$$\frac{H}{R} > \left(\frac{3\dot{m}}{\alpha\Delta t_S} \right)^{1/2} \frac{R^{3/4}}{(GM_{\text{BH}})^{1/4}} \sim 0.1 \frac{\dot{m}^{1/2} r_{0.1}^{3/4}}{\alpha_{0.1}^{1/2} \Delta_{0.01}^{1/2} m_7^{1/4}}. \quad (9)$$

In the last equality we define $\alpha_{0.1} \equiv \alpha/0.1$, $\Delta_{0.01} \equiv \Delta/0.01$, typical values for many models for α and observational constraints on Δ . Because $M_{\text{gas}} \sim 2\pi R^2 \Sigma$ and $\Sigma \sim 2\rho H$ in terms of the midplane gas density $\rho = \rho_{\text{mid}}$ of the disk, we immediately obtain a corresponding upper limit to the (volume-averaged) midplane density:

$$\rho_{\text{mid}} < \frac{G^{1/4} M_{\text{BH}}^{5/4} t_S^{1/2} \alpha^{1/2} \Delta^{3/2}}{4\sqrt{3}\pi R^{15/4} \dot{m}^{1/2}} \quad (10)$$

$$\lesssim \frac{5 \times 10^9 m_p}{\text{cm}^3} \left(\frac{m_7^{5/4} \alpha_{0.1}^{1/2} \Delta_{0.01}^{3/2}}{\dot{m}^{1/2} r_{0.1}^{15/4}} \right).$$

Notably, in the classic “ α -disk” model where α is a constant and the pressure is primarily thermal, $\Pi \sim \alpha P_{\text{tot}} \sim (0.01 - 0.1) P_{\text{thermal}} \sim (0.01 - 0.1)(\rho/m_p) k_B T_{\text{gas}}$ is (by assumption) dominated by thermal gas pressure in the outer disk, and the ratio $\Pi/\rho \propto T_{\text{gas}}$ depends *only* on the gas temperature. But the gas temperature in such models is set by the accretion rate itself – thus there is a robust constraint which does not allow any tunable parameters to resolve the key observational tensions we will discuss below.

3. OBSERVATIONS

Here we briefly review the compiled observations used to compare the models here, shown in Fig. 2 and listed in Table 1. We attempt to compile observations from a wide variety of objects using a number of different techniques, for several reasons. First, these allow us to probe different size scales and regimes of BH mass/luminosity. Second, they provide a

mutual consistency check that there are not large observational systematics biasing the conclusions. And third, they suggest that the results are representative of the general quasar population, not just populations which can be followed-up with a specific method. As we further discuss in § 5, the qualitative agreement of these different techniques, in samples spanning a range of BH mass and accretion rate, plus the fact that these samples do not appear to systematically deviate from “typical” AGN at similar luminosities in their continuum SED shapes (or other properties related directly to the accretion disk) suggest that they should be at least plausibly representative of the larger population.

The objects surveyed span BH masses $\sim 10^6 - 10^9 M_{\odot}$, and accretion rates/luminosities $L_{\text{bol}}/L_{\text{Edd}} \sim \dot{m} \sim 10^{-3} - 5$, with measurements at radii $R \sim 0.003 - 1$ pc ($\sim 4 - 5000$ ld, and $\sim 100 - 10^{7.5} R_G$ where $R_G \equiv GM_{\text{BH}}/c^2$), though the majority (and the most constraining cases) tend to reside around $M_{\text{BH}} \sim 10^7 - 10^8 M_{\odot}$, $\dot{m} \sim 0.1 - 1$, $r \sim 0.01 - 0.3$ pc ($10 - 1000$ ld, $\sim 300 - 10^{5.5} R_G$). In the sections below, we describe the model predictions for e.g. thermal, magnetic, turbulent, and radiation-pressure supported disks for the quantities V_c/V_K and $\partial \ln V_c / \partial \ln R$ shown in Fig. 2: these can be scaled for each model to the exact value of m_7 , \dot{m} , and R for each observation, and we discuss whether there are any other parameters in those specific models (like Q or α) that could improve agreement. We use the individual values in Table 1 for all quantitative comparisons and computation of the limits to e.g. H/R , ρ , Q (§ 2) and discuss them below, but for the sake of legibility in Fig. 2, we only plot reference model predictions for two representative variants of each of the four disk pressure assumptions ($\dot{m} \sim 0.1$ and ~ 1 , spanning the range of the most interesting observations).²

² There are a few systems in Table 1, namely NGC 4258, NGC 3783, J1339+1310, and J1206+4332, whose combination of BH mass, \dot{m} , and radii measured make them less-constraining for separating the models here at present.

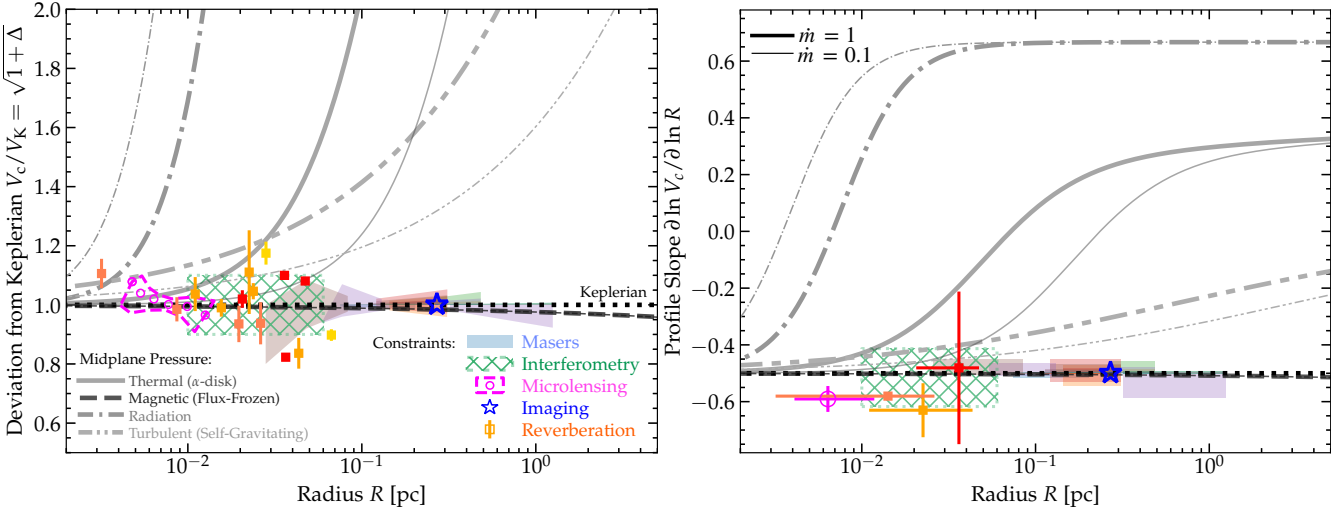


FIG. 2.— Observations (color; § 3), compared to the models (grayscale) per Fig. 1. We compile constraints from kinematics/rotation-curve-fitting from compilations of masers (shaded); GRAVITY optical interferometry of the BLR (hatched); microlensing response in broad-line wings (circles); plus individual resolved neutral-gas imaging and gas mass measurements in Circinus (star) and coordinated reverberation mapping of different BLR lines (squares). We compare model predictions assuming different midplane pressure sources as Fig. 1, for $\alpha = 0.1$, $m_7 = 1$ and $\dot{m} = 1$ (thick) or $\dot{m} = 0.1$ (thin). *Left:* Deviation from Keplerian circular velocities. *Right:* Logarithmic slope of the circular velocity curve, fitted to each over the range of measured velocities. The best masers are within $\sim 1\%$ of Keplerian, while the best BLR measurements constrain the profile to within $\sim 5 - 10\%$ of Keplerian, sufficient to rule out radiation or thermal-pressure dominated models, or turbulence-dominated models with $Q \lesssim 1$ at $r \gtrsim 0.003$ pc, but consistent with magnetic models at these radii. There is a hint of steeper-than-Keplerian curves in some BLR and maser systems, which only occurs in the magnetic models.

TABLE 1
SYSTEMS WITH PLOTTED DISK-MASS CONSTRAINTS.

Name	m_7	\dot{m}	R [pc]	Method	Reference
NGC 6323	1.00	1.4	0.14-0.31	Maser	Kuo et al. (2018)
UGC 3789	1.01	0.1	0.07-0.20	Maser	Kuo et al. (2018)
NGC 6264	2.66	0.1	0.26-0.48	Maser	Kuo et al. (2018)
NGC 5765b	4.87	0.04	0.30-1.3	Maser	Kuo et al. (2018)
NGC 2960 (Mrk 1419)	1.18	0.008	0.12-0.31	Maser	Kuo et al. (2018)
NGC 4258	3.83	0.0004	0.11-0.30	Maser	Kuo et al. (2018)
NGC 2273	0.75	0.15	0.03-0.09	Maser	Kuo et al. (2011)
J0437+2456	0.29	0.01	0.04-0.13	Maser	Gao et al. (2017)
ESO 558-G009	1.7	0.008	0.20-0.47	Maser	Gao et al. (2017)
NGC 5495	1.1	0.004	0.10-0.30	Maser	Gao et al. (2017)
Circinus	0.17	0.18	< 0.27	Imaging(+Maser)	Izumi et al. (2023)
Mrk 110	1.9	0.28	0.003-0.03	Reverberation	Kollatschny et al. (2001)
Mrk 817	3.8	0.19	0.01-0.04	Reverberation	Lu et al. (2021)
Mrk 509	10	0.16	0.03-0.07	Reverberation	Zu et al. (2011)
3C 390.3	51	0.07	0.02-0.05	Reverberation	Dietrich et al. (2012)
PDS 456	17	4.6	0.01-0.26	Interferometry	GRAVITY Collaboration et al. (2024)
3C 273	26	1.0	0.03-0.13	Interferometry	Gravity Collaboration et al. (2018)
IC 4329a	1.4	0.72	0.004-0.01	Interferometry	GRAVITY Collaboration et al. (2024)
Mrk1239	3.0	0.60	0.004-0.05	Interferometry	GRAVITY Collaboration et al. (2024)
Mrk 509	10	0.16	0.007-0.16	Interferometry	GRAVITY Collaboration et al. (2024)
IRAS 09149-6206	12	0.1	0.01-0.07	Interferometry	GRAVITY Collaboration et al. (2020)
NGC 3783	4.8	0.05	0.007-0.03	Interferometry	GRAVITY Collaboration et al. (2021)
J1004+4112	1.0	3.8	0.003-0.02	Microlensing	Fian et al. (2024)
J1001+5027	70	1.1	0.003-0.02	Microlensing	Fian et al. (2024)
HE 1104-1805	74	1	0.003-0.02	Microlensing	Fian et al. (2024)
J1206+4332	42	0.1	0.003-0.02	Microlensing	Fian et al. (2024)
J1339+1310	40	0.15	0.003-0.02	Microlensing	Fian et al. (2024)

For each AGN, we quote BH mass $m_7 \equiv M_{\text{BH}}/10^7 M_{\odot}$, accretion rate $\dot{m} = 0.1 \dot{M} c^2/L_{\text{Edd}}$, range of radii of the measured kinematic constraints, method, and reference from which the constraints are taken.

3.1. Masers

In many AGN, maser emission has enabled observational mapping of the kinematics and rotation curve of gas at radii ~ 0.01 –a few pc, most often around ~ 0.1 –1 pc surrounding black holes with masses $\sim 10^6$ – $10^8 M_{\odot}$ (Miyoshi et al. 1995; Greenhill et al. 1995; Braatz et al. 2004; Herrnstein et al. 2005; Henkel et al. 2005). This emission comes from molecular gas at densities $\sim 10^7$ – 10^{11} cm^{-3} and temperatures ~ 100 – 1000 K, at radii ~ 0.01 –1 pc (references above and

Modjaz et al. 2005; Kondratko et al. 2006a,b, 2008). Maser rotation curves have been extensively studied and modeled with sophisticated approaches that forward-model the observations directly from tilted-ring type assumptions allowing for different orbital anisotropy, eccentricity, warps, clumpiness, and other details. A common conclusion from these studies is that almost all maser rotation curves are at least consistent with a Keplerian potential (i.e. set some upper limit to Δ), and the most well-behaved and highest-signal-to-noise examples

set upper limits $\Delta \lesssim 0.01$ – i.e. reach percent-level sensitivity to deviations from a Keplerian potential (Moran et al. 1995; Läsker et al. 2016; Gao et al. 2017; Kuo et al. 2018; Linzer et al. 2022).

Here we compare the masers modeled in detail in Kuo et al. (2011, 2018); Gao et al. (2017). Specifically we take from their best-fit models the range of allowed deviations from Keplerian, including both their best-fit “BH+disk” models with the disk as a systematic deviation and the $\pm 2\sigma$ residuals with respect to the best-fit Keplerian model defined by the data therein. These are generally considered “high quality” masers, the most useful for our modeling here. Masers with more irregular kinematics can still place upper limits on Δ and therefore have constraining power (see § 3.4), but less so. We do not attempt to re-fit the datasets ourselves, but restrict to those with published detailed mass modeling.

As discussed below (§ 4.1.3), some maser lines allow strong constraints on the disk magnetic fields, via upper limits to Zeeman splitting. We compile and compare these as well, where relevant.

3.2. Torus-Scale Molecular Gas Imaging

In addition to maser measurements, ALMA has recently made it possible (in the nearest AGN) to obtain sub-pc resolved imaging and spectroscopy of neutral gas (molecular and atomic metal-lines). These allow for simultaneous kinematic constraints but also, where the kinematics are ambiguous or not sufficiently well-resolved, a direct census of the gas mass. In Circinus, a direct census of the total (technically neutral, but that is expected and predicted to dominate at these radii) gas mass from imagining gives $M_{\text{gas}} \sim 3500 - 6100 \text{ M}_{\odot}$ ($\sim 0.002 - 0.003 \text{ M}_{\text{BH}}$) at $r < 0.27 \text{ pc}$ (Izumi et al. 2023). Obviously $M_{\text{disk}} \lesssim M_{\text{gas}}$ (some of the gas could be outside the accretion disk), so this directly measures Δ and $M_{\text{gas}}(< R)$ at this point.

3.3. Broad-Line Regions

The broad line region (BLR) clouds are believed to be clouds orbiting in the vicinity of the supermassive black hole, at distances of $\sim 10^{-3} - 10^{-1} \text{ pc}$ (e.g., Peterson 2006; Hickox & Alexander 2018). Therefore, their observed velocities and distances from the supermassive black hole can be used to probe the gravitational potential well, and in particular, examine whether the kinematics are consistent with Keplerian motions caused by a single central point source mass. There are three types of BLR observations that probe the kinematics and spatial extents of the BLR clouds which we attempt to compile here: Reverberation Mapping (RM; see review by Cackett et al. 2021); imaging that directly resolves the BLR using interferometry (GRAVITY; e.g., Gravity Collaboration et al. 2018); and kinematic microlensing responses (microlensing; Vernardos et al. 2024) which are described below.

3.3.1. Reverberation Mapping

The BLR line fluxes are observed to vary in response to variations in the continuum emission with a short time delay (days to weeks; e.g., Kaspi et al. 2000; Peterson et al. 2004, and review by Cackett et al. 2021). This time delay is attributed to the light travel time across the BLR, and thus, represents the light-weighted distance of the line-emitting clouds from the continuum source. Since the continuum source, the accretion disk, is on much smaller scales of $\sim 10^{-5} - 10^{-3} \text{ pc}$, the time delay is considered to represent the distance from the

supermassive black hole. RM observations of several emission lines that trace gas at different ionization levels show that higher ionization lines, such as C IV and He II, have shorter time delays and broader Doppler widths, consistent with the idea that they trace gas that is orbiting closer to the supermassive black hole. In several well-studied systems such as NGC 5548, the different emission lines span a large-enough range in distance and show Doppler widths consistent with a $v \propto r^{-1/2}$ relation, the expected relation for Keplerian motions due to the supermassive black hole (e.g., Peterson & Wandel 1999; Bentz et al. 2009).

Most RM campaigns focus on mapping a single emission line (e.g., H α or H β) to obtain the size of the BLR. To test whether the motions are consistent with Keplerian motion, RM observations of several different ionization emission lines are required to probe different distances from the supermassive black hole simultaneously. Since the continuum emission may vary significantly over timescales of months-years, and due to the BLR size-luminosity relation, the different emission lines have to be observed over the same period of time. In addition, Fig. 1 shows that the Shakura & Sunyaev (1973) AD model is expected to diverge from Keplerian on scales of $\sim 0.03 \text{ pc}$. This implies that most BLR RM observations published in the literature, which target lower luminosity black holes with BLR sizes generally below 0.03 pc (e.g., Kaspi et al. 2000; Peterson et al. 2004; Bentz et al. 2009), cannot be used to test the models. BLR RM mapping of higher luminosity AGN require significantly longer observational campaigns, with very few published results for quasars (e.g., Lira et al. 2018). Nevertheless, a few higher luminosity cases have been observed with multiple emission lines (Mrk 817, 3C390.3, Mrk 509 and Mrk 110; see Kollatschny et al. 2001; Zu et al. 2011; Dietrich et al. 2012; Lu et al. 2021), and we show their derived velocities and distances in Fig. 2. In all but one case (Mrk 110), we use the line dispersion in the variable part of the spectrum to define the velocity, and the cross-correlation function centroid to define the time delay and thus the distance (see e.g., Peterson et al. 2004). Caution must still be taken when comparing these observations with model predictions, noting (i) the large uncertainties on the derived line kinematics, which also change with the ionizing luminosity during the campaign, and (ii) the assumption that each emission line represents a specific distance from the supermassive black hole. Finally, more recent, 2D RM campaigns suggest that the BLR motions in some sources are consistent with an outflow (see review by Cackett et al. 2021). Such analysis has only been applied to low-luminosity sources with BLR sizes lower than 0.03 pc , and thus they do not directly apply to Fig. 2.

3.3.2. Near-Infrared Interferometry

The second, more recent, observation that probes the BLR kinematics and geometry is direct imaging of the BLR clouds using long baseline near-infrared interferometry (GRAVITY; Gravity Collaboration et al. 2018). GRAVITY, a recently deployed instrument at the Very Large Telescope Interferometer in Chile, is capable of reaching a spectro-astrometric precision of micro arc-seconds, allowing it to spatially resolve the BLR clouds. In their first paper, Gravity Collaboration et al. (2018) identified a spatial offset between the red and blue photo-centres of the broad Pa α line of the quasar 3C 273. The detected spatial offsets and velocity gradients imply that the BLR gas is orbiting around the supermassive black hole, with their data well-fitted by a BLR model of a thick disk of gravitationally bound gas orbiting the black hole. We

present the spatial offsets and velocity gradients in Fig. 2. So far, GRAVITY had mapped the BLR of 7 objects in total, with derived BLR sizes between ~ 10 light-days (0.0084 pc) to ~ 300 light-days (0.25 pc; see [GRAVITY Collaboration et al. 2020, 2021, 2024](#)). These observations are fitted with an elaborate model of the BLR that includes a distribution of non-interacting clouds in a Keplerian/inflow/outflow motion, with varying spatial distributions in the r and θ directions, allowing the derivation of the black hole mass, the BLR mean size and thickness, and the BLR motion. The observations of five out of the seven sources are consistent with a rotating thick disk BLR, while the two others are consistent with outflow-dominated BLRs (Mrk 509 and PDS 456; [GRAVITY Collaboration et al. 2024](#)).

3.3.3. Microlensing

Third and most recently, [Fian et al. \(2024\)](#) attempted to reconstruct the circular velocity profile of five luminous quasars (SDSS J1001+5027, J1004+4112, J1206+4332, J1339+1310, & HE 1104-1805) from the microlensing response of different velocity components of the C IV and Si IV broad emission lines. Microlensing has been used to estimate the size of the AGN continuum-emitting and broad-line regions at different wavelengths, as the response function is smoothed and suppressed depending on the size of the emission region (see [Vernardos et al. 2024](#) for a review). [Fian et al. \(2024\)](#) find that reconstructing the sizes of different velocity components leads to a remarkably close-to-Keplerian circular velocity curve, in either C IV or Si IV and in either the blue or red wing of either line, for all five systems they study at $\sim 5 - 20$ light-days (below which they obtain primarily size upper limits). Note [Hutsemékers et al. \(2024b\)](#) argue that there is still non-trivial degeneracy in the models when an arbitrary distribution of broad-line emitter clouds plus microlensing objects is fitted, in particular that some (though not all) of the systems in [Fian et al. \(2024\)](#) can be comparably or better fit by “equatorial wind” as compared to rotating disk models. However: (1) per § 3.4 the functional form of the equatorial wind model in [Braibant et al. \(2017\)](#) and [Hutsemékers et al. \(2024a,b\)](#) – from [Murray et al. \(1995\)](#) – still assumes and implies a strictly Keplerian *potential*, simply that the gas is in a disk-like outflow geometry. And the deviations in the velocities which would appear if one introduced an additional disk mass to the potential have the *opposite* sense of the observational residuals they argue the wind model fits (i.e. they make the fit significantly worse). And (2) given our simplistic comparisons, our conclusions are identical if we restrict to the set of “cleaner” systems best-fit by the rotating disk models in [Hutsemékers et al. \(2024a,b\)](#).

3.4. Constraints on the Gravitational Potential versus non-Circular Motions

It is important to distinguish between the *circular velocity* V_c (Eq. 2), which by definition is a statement about the potential and enclosed mass, and the *rotation velocity* v_{rot} or line-of-sight projected mean velocity v_{los} of gas at some impact parameter b in projection from the SMBH. Gas can exhibit non-circular or non-Keplerian motions ($v_{\text{rot}} \neq V_c$) in a strictly Keplerian potential, owing to e.g. inflows/outflows, eccentric/radial motion, or clumpiness/turbulence. Detailed modeling can often disentangle these (see discussion in [Kuo et al. 2018; Gallimore & Impellizzeri 2023](#)), and various studies have found that almost all maser systems with apparently

non-Keplerian kinematics appear to be non-rotating (often impacted by outflows and/or jets; see references above and [Lonsdale et al. 2003; Henkel et al. 2005; Kuo et al. 2020; Panessa et al. 2020](#)). In these cases, what is measured still provides an upper limit to Δ , even if the magnitude of the fractional contribution of e.g. non-circular motion versus variation in the shape of the potential is unable to be determined. That, in turn, means that we still obtain a lower limit to P_{tot}/ρ – i.e. even these measurements are still able to give us a useful constraint. Of course, larger/less-strongly constrained upper limits to Δ are less constraining for our purposes. Similarly, at large radii (e.g. \gtrsim pc), there could be additional contributions to the potential or enclosed total mass M_{enc} from material besides the accretion disk or BH, including other (non-accreting) gas, stars, stellar-mass black holes, or dark matter. But again, given some observed rotation curve and upper limit on Δ , if there is any such contribution, then the accretion disk mass must be even lower than the limit derived above from Δ , and therefore P_{tot}/ρ would have to be even larger. So again because our constraints rely only on having a lower limit to P_{tot}/ρ , they are robust to these effects (if there is significant contribution to the potential from stars or dark matter or black holes, it would only strengthen our conclusions). But in either case the most interesting/useful constraints will come from observational cases which are closest-to-Keplerian, where the degeneracies of modeling/inferring V_c are minimized and where $\Delta \lesssim 0.01$ ([Kuo et al. 2018](#)).

To our knowledge, there are only two maser cases with acceptable fits³ which have been specifically argued by some as showing positive evidence of a non-Keplerian *potential*, NGC 3079 and 1068. We will discuss these specifically below in our comparisons and show that even taking the claimed detections at face value, the implied disk masses still rule out most disk models. But we would more generally argue these should still be treated as upper limits. For NGC 3079, the claim is fairly tentative – [Kondratko et al. \(2005\)](#) argue for some disk mass at < 0.7 pc, with a limit $M_{\text{disk}}^{3079} \lesssim 1 \times 10^6 M_{\odot}$ (with much larger uncertainties beyond that radius), but this system is well-known to have a bipolar jet/wind impacting the maser emission region directly, potentially producing irregular kinematics (the wind correction to the gravitational motions is order-unity). For NGC 1068 ($M_{\text{BH}} \sim 0.8 - 1.7 \times 10^7 M_{\odot}$, $\dot{m} \sim 0.2$), the most extreme claim of non-Keplerian motion comes from [Lodato & Bertin \(2003\)](#), who argue for an “additional” (non-BH) mass $M_{\text{disk}}^{1068} \lesssim M_{\text{non-BH}}^{1068} \sim 8 \times 10^6 M_{\odot} \sim M_{\text{BH}}$. But these authors still find an upper limit for the *slope* of the rotation curve $V_c \propto r^{\zeta_V}$ with $\zeta_V \leq 0$ (i.e. flat-or-declining V_c), which we will show rules out most thermal/radiation-pressure dominated disk models. And as they themselves note, there is clear evidence for at least some of this mass coming from stars in the nuclear star cluster (extrapolation of whose mass profile could account for all of the apparent

³ We exclude cases like NGC 7738, recently argued in [Ito et al. \(2025\)](#) to have $M_{\text{disk}} \gg M_{\text{BH}}$, as the best-fit model is statistically a poor fit to the data (reduced $\chi^2/\nu \equiv [N_i - N_{\text{model}}]^{-1} \sum_i (x_i - x_{\text{model}})^2 / \sigma[x_i]^2 \sim 3.9$, or as-fit $\chi^2_{\nu}/\nu \equiv [N_i - N_{\text{model}}]^{-1} \sum_i (v_i^{\text{los}} - v_{\text{model}}^{\text{los}})^2 / \sigma[v_i^{\text{los}}]^2 \sim 160$), indicating the fit is driven by more complex kinematics. Moreover that study utilized a linear χ^2 fit to $v_{\text{los}}(x_i)$, despite the dominant errors being in the maser positions x_i ; re-fitting their published data with a simple 2D maximum-likelihood model instead of a linear χ^2 gives a best-fit rotation curve slope completely consistent with Keplerian ($\partial \ln V_{\text{rot}} / \partial \ln R \rightarrow -0.57 \pm 0.11$ with $\chi^2/\nu \rightarrow 0.995$, as compared to the linear χ^2 fit $\partial \ln V_{\text{rot}} / \partial \ln R \rightarrow -0.14 \pm 0.04$ with $\chi^2/\nu \rightarrow 3.9 - 160$).

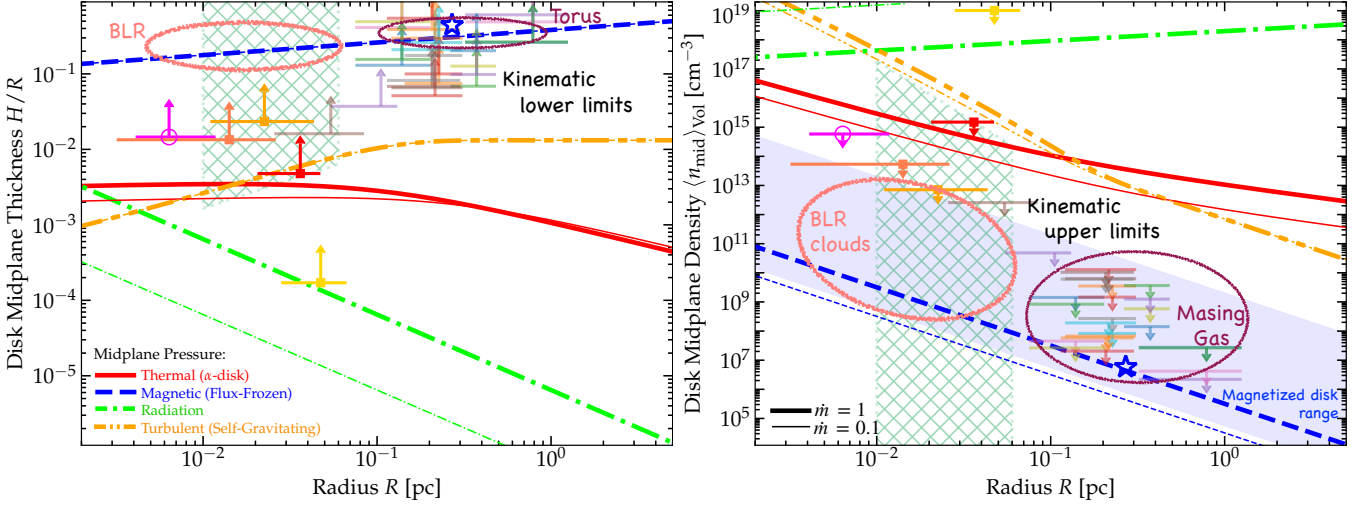


FIG. 3.— Corresponding predictions (as Fig. 1) and lower/upper limits (Eqs. 9–10) *purely from the kinematic constraints* in Fig. 2 on the central accretion disk scale-height H/R (top) and volume-averaged midplane density $\langle n_{\text{mid}} \rangle_{\text{Vol}}$ (bottom). These constraints do not depend on the tracers being “part of” the disk, only that they feel the gravitational potential of the disk (and therefore constrain its mass). For the magnetically-dominated disk, since the disks are predicted to be highly multi-phase, we show the expected range of densities (shaded). We also show (ellipses) the approximate typical height and radius range of the BLR and “torus” regions, from typical covering factors and resolved imaging, as well as the typical densities of BLR clouds and of maser gas (from spectral modeling). The kinematic constraints clearly favor the magnetized disk model at $\gtrsim 0.003$ pc. The limits on H/R and density imply that the BLR, masers, and torus do not “sit above” a much denser, thinner disk containing most of the mass, but rather are fundamentally part of the same structure.

rotation curve derivation), hence the upper limit $M_{\text{disk}}^{1068} \lesssim M_{\text{non-BH}}^{1068}$. Moreover, reanalysis with higher-resolution and more extensive datasets by [Gallimore & Impellizzeri \(2023\)](#) has argued that there is no evidence for non-Keplerian circular velocities (the feature in the observed velocities being driven by eccentric motions), and those authors set an updated upper limit $M_{\text{disk}}^{1068} < 10^5 M_{\odot}$.

4. CONSTRAINTS ON DIFFERENT PRESSURES

In Figs. 2–3, we compare the observed direct dynamical constraints on V_c/V_K (i.e. $M_{\text{disk}}/M_{\text{BH}}$), and correspondingly H/R and ρ , to different disk models. We immediately see that dynamical measurements rule out standard models of thermal-pressure, radiation-pressure, cosmic-ray pressure, and turbulence-only (with $Q \lesssim 1$) dominated disks, leaving magnetic-pressure dominated disks as the only viable option, at radii ~ 0.003 –3 pc (~ 4 –5000 light-days, or ~ 300 – $10^7 R_{\text{G}}$). In the following sections, we discuss this in more detail for each model in turn, and ask whether there is any adjustable model parameter which could alleviate these constraints. We further go into details on additional constraints and checks for each model (e.g. upper limits on the observed disk temperatures, luminosities, energetics, and magnetic field strengths), to support these conclusions.

4.1. Thermal-Pressure Dominated Disks (SS73)

4.1.1. The Standard α -Disk Is Immediately Ruled Out By Dynamical Constraints

If thermal pressure dominates, $P_{\text{tot}} \approx P_{\text{thermal}} = nk_B T = \rho c_s^2$. For disks with intermediate accretion rates ($0.001 \lesssim \dot{m} \lesssim 1$), the self-consistent accretion disk solution in this limit is that of SS73.⁴ It is straightforward to integrate that model, noting

⁴ Note that we will ignore radiatively inefficient, very-low \dot{m} optically-thin ADAF type solutions (e.g. [Yuan & Narayan 2014](#)) as we are interested in AGN accreting at modest luminosities. The classic super-Eddington “slim-disk” type extensions of SS73 ([Paczynsky & Wiita 1980; Abramowicz et al. 1988](#)) fall into the radiation-pressure dominated category, which we discuss below.

that by definition at the radii of interest we are well outside their regime “(a)” (radiation-pressure dominated), so we consider their regimes “(b)” (partially ionized, so scattering-opacity dominated) or “(c)” (more fully-neutral) therein, to obtain the predicted disk mass correction:

$$\frac{M_{\text{gas}}^{\text{therm}}(< R)}{M_{\text{BH}}} \sim \psi_{\text{therm}} \left(1 + \psi_{\text{therm}}^{1/4} \right) \quad (11)$$

$$\psi_{\text{therm}} \sim 1.2 \frac{\dot{m}^{7/10} r_{0.1}^{7/5}}{m_7^{1/5} \alpha_{0.1}^{4/5}} \text{MAX} \left[1, 0.8 \left(\frac{m_7}{r_{0.1}} \right)^{0.15} \right]$$

where the MAX in ψ reflects the regime (b)–(c) transition.

We also immediately obtain the related predictions:

$$\frac{H^{\text{therm}}}{R} \sim 0.004 \text{MIN} \left[\frac{\dot{m}^{1/5} r_{0.1}^{1/20}}{m_7^{3/20} \alpha_{0.1}^{1/10}}, \frac{\alpha_{0.1}^{1/4}}{(m_7 \dot{m})^{1/16} r_{0.1}^{9/16}} \right] \quad (12)$$

$$V_{c, \text{disk}}^{\text{therm}} \sim 740 \text{ km s}^{-1} m_7^{3/8} \dot{m}^{7/16} \alpha_{0.1}^{-1/2} r_{0.1}^{3/8} \quad (13)$$

$$T^{\text{therm}} \sim 2100 \text{ K} \times \text{MAX} \left[\frac{m_7^{11/20} \dot{m}^{3/10}}{r_{100}^{3/4} \alpha_{0.1}^{1/5}}, \frac{m_7^{5/8} \dot{m}^{5/8}}{r_{100}^{3/8} \alpha_{0.1}^{1/2}} \right] \quad (14)$$

$$n^{\text{therm}} \sim 1.5 \times 10^{13} \text{ cm}^{-3} \times \text{MAX} \left[\frac{m_7^{47/40} \dot{m}^{1/20}}{r_{100}^{15/8} \alpha_{0.1}^{7/10}}, \frac{m_7^{13/16} \dot{m}^{13/16}}{r_{0.1}^{11/16} \alpha_{0.1}^{5/4}} \right] \quad (15)$$

where $V_{c, \text{disk}}^{\text{therm}}$ refers to the contribution to V_c just from the disk self-gravity, and H^{therm} , T^{therm} , n^{therm} are the predicted scale-height/density/temperature from this model. We scale to the canonical $\alpha \sim 0.1$ for an SS73 disk though even $\alpha \sim 1$ (while already ruled out from other observational and theoretical constraints; see [Abramowicz & Fragile 2013](#)) would not change our conclusions.

These scalings are immediately ruled out by the constraints in Figs. 2–3 (rescaling for different $\alpha < 1$, m_7 , \dot{m} makes no difference, generally only making the discrepancies larger,

when we account for individual variations in these quantities between observed systems). In short, the model clearly predicts circular velocities exceeding Keplerian motions due to the black hole, with a rising rotation curve, i.e. $\Delta \gtrsim 1$ ($\gg 1$, at radii approaching ~ 1 pc), H/R much smaller than allowed by Eq. 9, as well as temperatures a factor ~ 20 larger than would permit molecular emission and gas densities $\sim 4 - 6$ orders of magnitude larger than the masing gas. And it predicts the disk is optically-thick to its own maser emission (with $\tau \gg 1$ even at \gtrsim pc radii), so the emission observed cannot possibly come from the disk. Even if somehow that gas were “not part of the disk” (in e.g. some “skin” above the disk, which somehow would have to be much colder while still being less dense, exactly the opposite of the SS73 predictions), the dynamics of the disk immediately strongly rule out such a model.

Not only does the thermal-pressure dominated model predict much too large a disk mass compared to what is allowed, but it also predicts a *rising* rotation curve, with $V_c \propto r^{+3/8}$ *increasing* with radius, much more steeply than even the most extreme allowed “disk-like” components observed (Lodato & Bertin 2003; Kondratko et al. 2005; Kuo et al. 2018).

To be specific, consider the claims of a “detection” (albeit indirect) of non-zero disk mass within the BHROI. In Circinus, a direct census of the total (neutral, but that is expected and predicted to dominate at these radii) gas mass from imagining gives $M_{\text{disk}}^{\text{Circ}} \sim 3500 - 6100 M_{\odot}$ ($\sim 0.002 - 0.003 M_{\text{BH}}$) at $r < 0.27$ pc (Izumi et al. 2023). For its BH mass and accretion rate (tabulated below, but well into the regime $\dot{m} \sim 0.1$ where these predictions and model comparisons should apply), the prediction from this model is $M_{\text{disk}}^{\text{therm}} \sim 5.2 \times 10^6 M_{\odot}$ – one thousand times larger than observed. Next consider NGC 1068 ($M_{\text{BH}} \sim 0.8 - 1.7 \times 10^7 M_{\odot}$, $\dot{m} \sim 0.2$), perhaps the most well-studied BH where some have claimed maser evidence for a non-Keplerian rotation curve from disk self-gravity. The most extreme such claim from Lodato & Bertin (2003) argues that the upper limit for the *slope* of the rotation curve is flat, i.e. $V_c \propto r^{\zeta_V}$ with $\zeta_V \leq 0$, while the model here predicts $+3/8$, clearly ruled out. And their inferred disk mass is $M_{\text{disk}}^{1068} \lesssim 8 \times 10^6 M_{\odot}$: but for these parameters the thermal-pressure dominated models predict $M_{\text{disk}}^{\text{therm}} \approx 4 \times 10^8 M_{\odot}$, a factor 100 larger than observationally claimed. And as noted in Lodato & Bertin (2003), there is clear evidence for at least some of this “disk” mass coming from stars in the nuclear star cluster (extrapolation of whose mass profile could account for all of the apparent rotation curve derivation), hence the upper limit here. Moreover for this particular case, re-analysis with higher-resolution and more extensive datasets by Gallimore & Impellizzeri (2023) has argued that there is no evidence for non-Keplerian circular velocities (the feature in the observed velocities being driven by eccentric motions), and those authors set an updated upper limit $M_{\text{disk}}^{1068} < 10^5 M_{\odot}$, which is more than 1000 times smaller than the thermal disk predictions. NGC 3079 may also have a massive disk (Kondratko et al. 2005), but also is well-known to have a bipolar jet/wind impacting the maser emission region directly, potentially producing irregular kinematics (the wind correction to the gravitational motions is order-unity). Still Kondratko et al. (2005) argue for some disk mass at < 0.7 pc, with a limit $M_{\text{disk}}^{3079} \lesssim 1 \times 10^6 M_{\odot}$ (with much larger uncertainties beyond that radius). But again, the thermal disk model for the parameters of 3079 predicts $M_{\text{disk}}^{\text{therm}} \sim 1.3 \times 10^8 M_{\odot}$ at this radius, a factor > 100 times larger than allowed. And in essentially

all other cases, the upper limits to the disk mass are much lower (more like our default-scaled $\Delta \sim M_{\text{gas}}/M_{\text{BH}} \lesssim 0.01$; Kuo et al. 2018). Thus even the most extreme claims of detected self-gravitating accretion disks, taken at face value, are multiple orders-of-magnitude less massive than the disk masses predicted if the disks were thermal-pressure dominated or SS73-like.

4.1.2. Any Other Thermal-Pressure-Dominated Disk Is Also Ruled Out

What if we completely ignored the physics used to derive the classic α -disk model above (i.e. physically-self-consistent opacities and temperature structure, the assumption that the disk is optically thick, even basic physical constraints like energy conservation), and simply allowed the disk to have $P_{\text{tot}} \approx P_{\text{thermal}}$ with any temperature (i.e. simply “fit” a temperature to be consistent with Eq. 7)? In this limit, our constraint on Δ through Eq. 7 immediately translates to a lower bound on T :

$$T^{\text{therm}}(R) \gtrsim 10^6 K \frac{\dot{m} m_7^{1/2} r_{0.1}^{1/2} \mu_m}{\alpha_{0.1} \Delta_{0.01}} \quad (16)$$

This can be immediately ruled out for several reasons. Theoretically, (1) it is impossible to sustain – at these temperatures the disk would cool far too efficiently and the cooling rate at these radii would be orders-of-magnitude larger than the gravitational energy flux (this is just the statement that the disk could *not* be self-consistent); and (2) at these temperatures and radii one could not avoid radiation pressure becoming larger than thermal. But more importantly, purely observationally, we know (1) this temperature is far too hot to allow maser emission to exist; (2) this is also far hotter than the thermal emission temperature from the BH (from the spectrum of the big blue bump); and (3) this would necessarily imply an unphysically large luminosity from the gas at these radii. For the latter, taking $L(R) \approx 4\pi\sigma_B T_{\text{eff}}^4$ as the luminosity from each annulus R , consistent with the regime that the disk would have to be in here, and comparing this to the Eddington limit, Eq. 16 implies:

$$\frac{L^{\text{therm}}(R)}{L_{\text{Edd}}} \gtrsim 10^{11} m_7 \left(\frac{\dot{m} r_{0.1} \mu_m}{\alpha_{0.1} \Delta_{0.01}} \right)^4 \quad (17)$$

i.e. more than 10 orders of magnitude larger than observed! Moreover $L(R)$ increases as R^4 , implying almost all the observed quasar emission comes from $>$ pc scales, which is clearly ruled out by both variability and direct imaging constraints.

Thus completely independent of assumptions for α or details of the accretion disk structure, we can immediately observationally rule out that the disks *at the radii of maser/outer-BLR/dust emission* are thermal-pressure dominated.

4.1.3. Constraints from Zeeman Observations on Magnetic Field Strengths

In the “arbitrary” thermal-pressure dominated models, we have no prior for the magnetic field strengths. But of course in the classic, physically-motivated and widely-used SS73 or α -disk models, the stress $\alpha \neq 0$ directly reflects the magnetic stresses in the disk (generally believed to arise from e.g. the magnetorotational instability [MRI] in the disk), with $\alpha \sim |\langle B_{\phi} B_R \rangle|/(4\pi\rho c_s^2) \lesssim \langle B_{\phi}^2 \rangle/(4\pi\rho c_s^2)$ (Shakura & Sunyaev 1973; Balbus & Hawley 1998; Balbus 2003) (note this also

TABLE 2
DIRECT MASER CONSTRAINTS ON IN-PLANE B .

Name	m_7	\dot{m}	$B_{\parallel}^{\text{lim}}$ [mG]	R^{lim} [pc]	Reference
NGC 3079	0.2	0.1-0.5	33	0.64	Vlemmings et al. (2007)
NGC 4258	4	$10^{-(3.5-4)}$	30-90	0.14-0.27	Modjaz et al. (2005)
NGC 1194	6.5	0.02	100	0.6	Pesce et al. (2015)
NGC 2273	0.8	0.06	160	0.5	Pesce et al. (2015)
NGC 3393	3.1	0.04	300	0.5-1.5	Pesce et al. (2015)
NGC 6323	0.9	0.1	300	0.2	Pesce et al. (2015)
NGC 2960	1.2	0.05	720	0.35	Pesce et al. (2015)
ESO 558-G009	1.8	>0.007	310	0.7	Pesce et al. (2015)
Circinus	0.17	0.2	150-360	0.1-0.4	McCallum et al. (2007)

For each AGN, we quote BH mass m_7 , accretion rate \dot{m} , claimed upper limit $B_{\parallel}^{\text{lim}}$ (3σ or limit available from reference) to in-plane B_{ϕ} or $|B_{\parallel}|$ in mG, and radius R in pc where the upper limit is measured, from the given references.

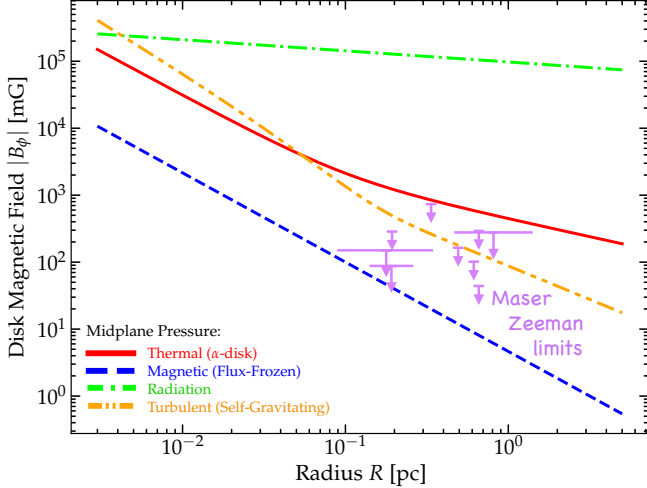


FIG. 4.— Corresponding predictions as (Fig. 1) for the midplane in-plane magnetic field strengths ($|B_{\phi}|$) (assuming a Maxwell stress comparable to Reynolds/accretion stress for each model). We overplot upper limits from maser Zeeman constraints (Table 2). Magnetically-dominated disks actually predict the weakest absolute $|\mathbf{B}|$ of any of the models, owing to their much lower overall densities (Fig. 3). This appears to be clearly favored by the maser constraints at $\gtrsim 0.1$ pc.

includes contributions from Reynolds stresses, but these are fixed in ratio and modestly sub-dominant in saturated MRI turbulence; Pessah et al. (2006). So we can estimate a minimum toroidal magnetic field strength predicted by these models (as did SS73), giving:

$$B_{\phi}^{\text{therm, pred}} \gtrsim 1.5 \text{G} \times \text{MAX} \left[\frac{m_7^{69/80} \dot{m}^{17/40} \alpha_{0.1}^{1/20}}{r_{0.1}^{21/16}}, \frac{m_7^{23/32} \dot{m}^{23/32}}{r_{0.1}^{17/32} \alpha_{0.1}^{3/8}} \right] \quad (18)$$

This is quite large, and potentially in tension (though much less dramatically so than the disk mass constraints above) with observational constraints from Zeeman splitting in masers, summarized in Table 2 and shown in Fig. 4. We focus on direct maser Zeeman detections or upper limits here, since these provide a more or less model-independent upper limit to B_{ϕ} most robustly, as compared to methods like those in Silant'ev et al. (2010); Piotrovich et al. (2021) for inferring “disk magnetic field strengths” which (1) are sensitive to measurements coming from radii near-horizon (near the jet-launching region) and (2) are highly model dependent (e.g. *assuming* SS73 to

infer $|\mathbf{B}|$ from other properties like the accretion rates and spectral shape). Restricting to the direct maser constraints, we find specifically for (NGC 3079, 4258, 1194, 2273, 3393, 6323, 2960, ESO 558-G009, Circinus) the predicted $|B_{\parallel}^{\text{therm}}|$ are $\sim (33-110, 30-110, 140, 72, 80-150, 210, 100, 24, 64-170)$ mG from Eq. 18. A couple of these (e.g. 3079, noting that the Vlemmings et al. 2007 upper limit is already a 3σ upper limit and corresponds to the lower end of this predicted range for the lowest allowed accretion rates for this object) appear significant at the $2-3\sigma$ level, but they are nowhere near as unambiguous as the mass comparisons above.

4.2. Magnetic-Pressure Dominated Disks (Hyper-Magnetized, Flux-Frozen Disks)

4.2.1. Agreement with Observed Dynamical Constraints on Disk Mass Profiles

What if instead the disk were magnetic pressure dominated, so $P_{\text{tot}} \approx P_{\text{mag}} = B^2/8\pi \sim (1/2) \rho v_A^2$? For disks in this regime, the self-consistent model for structure assuming $P_{\text{tot}} \approx P_{\text{mag}}$ with magnetic field strengths determined by flux-freezing is presented in Hopkins et al. (2024c). This gives the prediction

$$\frac{M_{\text{gas}}^{\text{mag}} (< R)}{M_{\text{BH}}} \sim 10^{-3} \frac{\dot{m} r_{0.1}^{7/6} r_{ff,5}^{1/3}}{\alpha_{0.1}^2 m_7^{1/2}} \sim 10^{-5} \frac{\dot{m} r_{0.1}^{7/6}}{\alpha^2 m_7^{1/3}} \quad (19)$$

(here our parameter α serves the same role as the parameter ψ in Hopkins et al. 2024c). This is orders-of-magnitude smaller than $M_{\text{gas}}^{\text{therm}}$, because the Maxwell stresses and turbulence are much stronger than an SS73 disk which is limited by $P_{\text{mag}} \sim P_{\text{turb}} \ll P_{\text{therm}}$. Obviously this is easily allowed by present constraints on Δ , for any reasonable α , and we see this plainly in Figs. 2-3.

Even considering the couple of systems for which a claimed disk mass is detected from § 4.1.1, the magnetized models appear more consistent with the observations. For Circinus, recall the direct imaging of neutral gas mass gives $M_{\text{disk}}^{\text{Circ}} \sim 3500-6100 M_{\odot}$ at $r < 0.27$ pc (Izumi et al. 2023). The prediction from Eq. 19 for the same BH mass and accretion rate is $M_{\text{gas}}^{\text{mag}} \sim 3000 \alpha_{0.1}^{-2} M_{\odot}$, in remarkably good agreement for a Maxwell stress approximately equal to $\sim 10\%$ of the total magnetic pressure (very similar to that predicted in the simulations in Hopkins et al. 2024b). The more extreme, albeit indirect claims from kinematics for NGC 1068 and 3079 (Lodato & Bertin 2003; Kondratko et al. 2005) are larger than the predicted disk mass from Eq. 19 by factors of 10-100.

However, as noted by those authors themselves as well as [Kuo et al. \(2018\)](#), there are alternative explanations, for example that the deviation from a Keplerian rotation curve is caused by stellar mass becoming significant interior to ~ 1 pc in these systems, or the known irregular kinematics of the jet/wind system in 3079. In these cases the claimed disk masses should be treated as upper limits, making the prediction of Eq. 19 consistent with the observations. And indeed [Gallimore & Impellizzeri \(2023\)](#) revisited 1068 with higher-resolution and more extensive datasets and argued $M_{\text{disk}}^{1068} < 10^5 M_{\odot}$, completely consistent with Eq. 19 but smaller by a factor of ~ 1000 than the predictions for any thermal-pressure dominated disk (§ 4.1.1). They note that the apparent deviations from Keplerian rotation are more consistent with a coherent eccentric mode with a few-percent amplitude, exactly the sorts of modes that appear to be ubiquitous in magnetically-dominated disks (see the examples in [Hopkins et al. 2024a,b](#)).

Briefly, we note that sometimes it has been argued that spiral or eccentric structure in an accretion disk implies significant disk self-gravity ([Maoz 1995](#); [Gallimore & Impellizzeri 2023](#)), but this is incorrect. It has been known for decades that even in the test-particle limit of *zero* self-gravity in a perfectly Keplerian potential, strong spiral and/or eccentric modes can easily be powered *directly* by the MRI ([Heinemann & Papaloizou 2009](#)) or by other non-axisymmetric magnetic modes in non-self-gravitating but strongly magnetized disks ([Das et al. 2018](#)), or seeded by random fluctuations in disks with strong magnetic fields (see references in [Hopkins et al. 2024a,b](#)), or can propagate in from $R = \infty$ (much larger radii where self-gravity may not be negligible) without any barrier ([Adams et al. 1989](#); [Tremaine 2001](#); [Jacobs & Sellwood 2001](#); [Touma 2002](#); [Bacon et al. 2001](#); [Hopkins & Quataert 2011b](#); [Hopkins 2010](#); [Hopkins & Quataert 2011a](#)). And indeed such modes are ubiquitously seen in simulations with non-linearly large amplitudes even when self-gravity is disabled in the simulations (see [Hopkins & Quataert 2010b,a](#); [Hopkins et al. 2016](#); [Gaburov et al. 2012](#); [Jiang et al. 2019](#); [Kudoh et al. 2020](#); [Davis & Tchekhovskoy 2020](#); [Kaaz et al. 2023](#)). So existence of even non-linearly high-amplitude spiral structure or eccentric orbits does not imply any meaningful constraint, in and of itself, on the mass of the accretion disk.

From the same magnetically-dominated accretion disk models in [Hopkins et al. \(2024c\)](#), we immediately obtain the related predictions for the mean density $n \sim 10^6 m_7^{3/4} \dot{m} r_{0.1}^{-2} \alpha^{-3}$, but note that the disk is necessarily supersonically turbulent and multiphase so the dense gas has densities between this and $n (v_{\text{turb}}/c_s)^2$ or $n \sim (10^6 - 10^{10}) \alpha^{-3} \text{ cm}^{-3}$ (see [Hopkins et al. 2024a,b](#); [Hopkins 2025](#)). The model also predicts $\tau \lesssim 1$ for both scattering and absorption of the maser and BLR emission at these wavelengths at all radii \gg light-days, and at maser radii ~ 0.1 pc temperatures $T \sim T_{\text{eff}} \sim 200 - 1000$ K at ~ 0.1 pc ([Hopkins et al. 2024a](#); [Hopkins 2025](#)), depending on whether we consider the colder more-shielded midplane or partially-illuminated surface layers. And the disk is thick and flared, with $H/R \sim \alpha m_7^{-1/12}$ ([Hopkins et al. 2024c,b](#)). More detailed comparisons are in [Hopkins et al. \(2024a,b\)](#) and (Baradai et al., in prep.), but at the order-of-magnitude level, this is remarkably consistent with both the properties of maser gas at $\sim 0.1 - 1$ pc and BLR emitting gas at $\sim 1 - 100$ ld ($\sim 0.001 - 0.1$ pc).

4.2.2. Effects of Pressure Support at Large H/R

For these magnetized disks, H/R is sufficiently large ($\gtrsim 0.1$) that one might worry about pressure support causing non-Keplerian motion, even in the test particle limit (i.e. the asymmetric drift correction being large). Generically, for a magnetically-supported disk, this gives:

$$V_{\text{rot}} \approx v_c \sqrt{1 + \frac{1}{\rho v_c^2} \frac{\partial P_{\text{eff}}}{\partial \ln R}} \approx v_K \left[1 + \frac{h^2}{2} \left(1 + \frac{\partial \ln B_\phi}{\partial \ln R} \right) \right] \quad (20)$$

where $h = H/R \approx v_A/2 v_K$. Importantly, if $H/R \sim \text{constant}$ or $\partial \ln B_\phi / \partial \ln R \approx -1$, there is *no* measurable correction: the shape of the rotation curve is exactly Keplerian at all r (just with a potentially slightly different normalization, which is degenerate with a slightly different BH mass). But in the analytic models in [Hopkins et al. \(2024c\)](#) and simulations in [Hopkins et al. \(2024a,b\)](#), both of these conditions are approximately true: the favored models give H/R varying between constant ($\propto R^0$) and $\propto R^{1/6}$, and $-4/3 \leq \partial \ln B_\phi / \partial \ln R \leq -1$. So in practice calculating the expected non-Keplerian motions from pressure support from *any* of the analytic family of models in [Hopkins et al. \(2024c\)](#) or the simulations in [Hopkins et al. \(2024a,b\)](#) gives deviations from v_K below percent-level.

Moreover, even those (very weak) effects are quite distinct from the upper limits to increasing V_c we are focused on here. Because the disk can flare (H/R increases with R and $\partial \ln B_\phi / \partial \ln R \leq -1$), this predicts a very slightly *steeper* decline of V_{rot} with R than Keplerian, meaning that the sense of the deviations predicted is actually *more* consistent with the upper limits in the literature. In practice this deviation is basically undetectable: over a 1 dex range from $\sim 0.1 - 1$ pc for a $\sim 10^7 M_{\odot}$ BH, the favored model from [Hopkins et al. \(2024c\)](#) with the maximal deviation ($\partial \ln B_\phi / \partial \ln R = -4/3$) gives a rotation curve which would be formally best-fit by $v_{\text{rot}} \propto r^{-0.505}$ instead of $r^{-0.5}$, well within observational uncertainties. We can also confirm this directly in the full global simulations of [Hopkins et al. \(2024b\)](#). There, the deviations predicted from the magnetic pressure support are similarly unmeasurably small (not surprising, since the analytic scaling of the favored model in [Hopkins et al. 2024c](#) is a good fit to the simulations in [Hopkins et al. 2024b](#)), smaller than this upper limit (since H/R is slightly closer to constant, see Fig. 5 in [Hopkins et al. 2024b](#)). There there are much larger deviations at these radii from Keplerian driven by eccentric motions in the disk: evidence for these is also commonly seen in maser disks (see discussion above), but of course this has nothing to do with the mass profile and enters differently from the disk mass limits above (in how it modifies the apparent rotation curve, since it causes a global asymmetry) and therefore does not change any of our conclusions here.

Note the $1 + \partial \ln B_\phi / \partial \ln R$ term in Eq. 20 and vanishing of the corrections to Keplerian motion for $B_\phi \propto R^{-1}$ arises because of the competing magnetic tension and pressure terms in B_ϕ in the radial momentum equation. Such cancellation is not possible for e.g. a thermal or radiation-pressure dominated disk, which would predict much larger deviations from Keplerian orbits if H/R were large. So again, the nearly-Keplerian behavior observed further favors magnetically-dominated disks.

4.2.3. Measurement of Magnetic Field Strengths from Maser Zeeman Splitting

As in § 4.1.3, we can also attempt to compare the predicted in-plane magnetic field strengths from these models directly to the maser Zeeman upper limits compiled in Table 2. From the same models giving Eq. 19 (Hopkins et al. 2024c), we have the predicted:

$$B_\phi^{\text{mag, pred}} \sim 0.1 \text{G} \frac{m_7^{19/24} \dot{m}^{1/2}}{\alpha^{1/2} r_{0.1}^{4/3}} \quad (21)$$

For (NGC 3079, 4258, 1194, 2273, 3393, 6323, 2960, ESO 558-G009, Circinus) the predicted $|B_{\parallel}^{\text{mag}}|$ are $\sim (0.7 - 1.7, 0.8 - 3.4, 5.7, 2.4, 1.3 - 5.7, 12, 4.9, 1.0, 1.7 - 11) \alpha^{-1/2}$ mG, all well below the observed upper limits even for rather low α . We can also compare to the Lopez-Rodriguez et al. (2013) estimate of $|\mathbf{B}|$ from polarization on “torus” scales in IC 5063 ($m_7 \sim 28$; $\dot{m} \sim 0.02 - 0.1$), with $|B_{\parallel}| \sim 12 - 130$ mG inferred from polarization of an unknown hot dust emitting region at < 250 pc, probably associated with the dust sublimation radius at ~ 1 pc as argued by Lopez-Rodriguez et al. (2013), where Eq. 21 would predict $|B_{\parallel}^{\text{mag}}| \sim (9.2 - 20) \alpha^{-1/2}$ mG (for the uncertain range of \dot{m} quoted above), reasonably consistent for a plausible range of α .

From comparison of Eq. 18 & 21, more explicitly in Fig. 4, we can immediately see the important point emphasized in Hopkins et al. (2024c) and Hopkins et al. (2024b). Namely, that the in-plane B_ϕ or B_{\parallel} is actually *smaller*, for the same BH mass and accretion rate, in the magnetically-dominated models as compared to the thermal-pressure-dominated models. This occurs because the thermal-dominated models are so much thinner and higher-surface density (owing to low temperatures making the upper limit to the stress Π very small, hence requiring a large mass to support even a modest accretion rate), that their physical 3D midplane densities ρ are many orders of magnitude larger than those predicted by the magnetically-dominated disk models, and so maintaining even a small Alfvén speed or Maxwell stress in those thermal-dominated models requires an order-of-magnitude larger absolute value of $|\mathbf{B}|$.

4.3. Radiation-Pressure Dominated Disks

Now consider a radiation-pressure dominated disk, $P_{\text{tot}} \approx P_{\text{rad}}$. The standard radiation-pressure dominated solution requires the disk be optically-thick, but it also becomes strongly turbulent which removes strong stratification, giving $P_{\text{rad}} \sim (4\sigma_B/3c) T_{\text{rad}}^4 \sim (4\sigma_B/3c) T_{\text{eff}}^4$. The standard “self-consistent” solutions given in either Shakura & Sunyaev (1973) or Abramowicz et al. (1988) give a similar predicted scaling:

$$\frac{M_{\text{gas}}^{\text{rad}}(< R)}{M_{\text{BH}}} \sim 400 \frac{r_{0.1}^{7/3}}{m_7^{5/3} \dot{m}^{2/3} \alpha_{0.1}^{2/3}} \quad (22)$$

with $V_c \propto r^{+2/3}$, which can be immediately ruled out in Figs. 2-3.⁵

⁵ At much smaller radii where the disk mass eventually becomes smaller than the BH mass, this model predicts $M_{\text{gas}}/M_{\text{BH}} \sim 5300 r_{0.1}^{7/2} m_7^{-5/2} (\dot{m} \alpha_{0.1})^{-1}$, but that would only apply at radii interior to $r \ll 0.007$ pc ($\alpha_{0.1} \dot{m}$)^{2/7} $m_7^{5/7}$, well interior to the radii of interest here, and moreover even then this scaling would still be ruled out by $\Delta_{0.01} \sim 1$ (nearly-Keplerian rotation), down to even smaller radii $r \lesssim 1 (\alpha_{0.1} \dot{m})^{2/7} m_7^{5/7}$ light-day, interior to the BLR.

More generally, a radiation-pressure supported disk, by definition, $\kappa F/c = g \approx \Omega^2 H$, so if we define the luminosity $L(R) \approx 2\pi R^2 F$ as above and the usual $L_{\text{Edd}} = 4\pi G M_{\text{BH}} m_p c / \sigma_T$, our constraint becomes:

$$\frac{L(R)}{L_{\text{Edd}}} \gtrsim \frac{H/R}{\kappa/\kappa_{\text{es}}} \gg 0.1 \frac{\dot{m}^{1/2} r_{0.1}^{3/4}}{\alpha_{0.1}^{1/2} \Delta_{0.01}^{1/2} m_7^{1/4}} \frac{\kappa_{\text{es}}}{\kappa} \quad (23)$$

Thus unless $\kappa \gg \kappa_{\text{es}}$, it is not possible to hold up the disk and obey the observed constraints without producing far more radiation than observed, with *most* of the radiation coming from large radii, and being vastly colder than observed (characteristic radiation temperatures $\lesssim 1000$ K). This is clearly ruled-out observationally but is also unphysical, since there is nothing that could power such large luminosities at large radii (it is many orders-of-magnitude larger than the accretion luminosity).

Even if one invokes large dust opacity at the very largest radii \gtrsim pc, it would not in general bring $L(R)$ required here below observational limits. But for many inner maser regions, the dust is clearly sublimated (there is nowhere near as much dust observed as there would be if it were not). If the dust is sublimated and the gas atomic/molecular with observed maser temperatures $\ll 10^4$ K, then the maximum opacity is $\kappa \sim \kappa_{\text{mol}} \sim 0.001 (Z/Z_{\odot})$, so we have $L(R) \gtrsim 100 L_{\text{Edd}} r_{0.1}^{3/4}$ – i.e. the observed luminosities immediately rule out a radiation-pressure supported disk. More rigorously, since the masering radii cannot be optically-thick to self-absorption (or they would not be observed as they are), we can set a strong upper limit on their opacity at their radii, giving $\kappa/\kappa_{\text{es}} \ll 0.02 / [(H/R) n_8 r_{0.1} \mu_{\text{mol}}]$ for a masering gas density $n = n_8 10^8 \text{ cm}^{-3}$, which means we *must* at a maser radii have

$$\frac{L(R)}{L_{\text{Edd}}} \gg 0.5 \frac{\dot{m} n_8 R_{0.1}^{5/2}}{m_7^{1/2} \alpha_{0.1} \Delta_{0.01}} \quad (24)$$

in order to have a radiation-pressure supported disk. Again, this is immediately ruled-out.

4.4. Turbulent Ram-Pressure Dominated Disks

4.4.1. Allowed Strength of Turbulence and Conceivable Drivers in the Absence of Any Other Dominant Pressure

In simulations and models of both magnetic and radiation-pressure dominated disks, the predicted turbulence is broadly near equipartition with these energy sources (Jiang et al. 2019; Hopkins et al. 2024b). So, given that the magnetic pressure-dominated models appear completely consistent with observational constraints (§ 4.2), it is perfectly plausible that turbulence could be an $\mathcal{O}(1)$ component of the “required” disk support. We can see this directly from Eq. 7 with $\Pi \sim \alpha P_{\text{tot}} \sim \alpha P_{\text{turb}} \sim \alpha \rho v_{\text{turb}}^2$, the turbulent velocity must only exceed:

$$v_{\text{turb}} \gtrsim 20 \text{ km s}^{-1} \frac{\dot{m}^{1/2} m_7^{1/4} r_{0.1}^{1/4}}{\alpha^{1/2} \Delta_{0.01}^{1/2}} \quad (25)$$

This is much smaller than v_K , and completely allowed by the more detailed kinematic and dynamical modeling of line dispersions/widths from maser and BLR imaging (not just the rotation curves in Figs. 2-3).

TABLE 3
SUMMARY OF PREDICTIONS OF DIFFERENT ACCRETION DISK PRESSURE SOURCES.

Dominant Pressure	Slope $V_c \propto R^{\zeta_V}$		Observational Contradiction	Theoretical Contradiction
Radiation	$\zeta_V \sim +2/3$ (steeply-rising)	$L_{\text{outer disk}}$	$\gg L_{\text{Edd}}$ always, most luminosity from $\gtrsim 1$ pc	No physical radiation source
Thermal	$\zeta_V \sim +3/8$ (steeply-rising)	$L_{\text{outer disk}}$	$\gg L_{\text{Edd}}$ always, $T_{\text{spec}} \gg 10^6$ K (spectra super-hot)	No physical heating source
Cosmic Ray	No consistent model		γ -ray luminosity $L_{\gamma} \gtrsim L_{\text{Edd}}$	No sufficient CR source
Gravitoturbulence	$-0.25 < \zeta_V < 0$ (flat or slow-falling)	Requires $Q \sim 100$, not $Q \sim 1$; no single Q fits H/R & M_{disk}		What drives the turbulence?
Magnetic	$-0.55 \lesssim \zeta_V \lesssim -0.5$ (near-Keplerian)		None	None

For each row, we assume the pressure holding up the accretion disk at large radii ($\gg 0.01$ pc) comes primarily from the given source. Columns: (1) Pressure source. (2) Shape of the rotation curve at these radii. (3) Other immediate contradictions with observations this would predict, if we forced the parameters (e.g. T , L , etc.) to have values consistent with the maser kinematics. (4) Theoretical contradictions if one attempts to support the disk with such pressure.

So turbulent pressure being of order P_{tot} , as a statement in and of itself, is allowed by the constraints in Figs. 2-3. But the question relevant for this section here is: “Can the disk be supported *entirely* by turbulence?”. In other words, can one have $P_{\text{tot}} \sim P_{\text{turb}}$ with no *other* large pressure of the forms already reviewed, i.e. thermal, magnetic, radiation, cosmic ray, and other pressures all much smaller than turbulent? This means the turbulence would necessarily be highly supersonic and super-Alfvénic, which in turn means its dissipation time must be of order the crossing/turnover time $t_{\text{diss}} \sim H/v_{\text{turb}} \sim \Omega$ (if it is supporting the disk in the first place). So since it *must* dissipate, by definition, on a timescale faster than the accretion time, it must also therefore be “powered” by something. But by definition in this regime the power source cannot be the thermal, magnetic, radiation, cosmic ray, neutrino, or chemical energy of the disk. That leaves only two energy sources which have been discussed in the literature: feedback from massive stars within the disk (e.g. SNe, radiation, stellar mass-loss) and gravity. Note that feedback from the central accretion disk would not vertically support the disk, and if it had the form of a wind, would change the rotation curves, and if it acted via radiation/cosmic ray acceleration/thermal heating would violate our requirement of $P_{\text{tot}} \sim P_{\text{turb}}$ alone.

4.4.2. Stellar Feedback-Driven Turbulence Is Ruled Out on These Scales

Feedback from stars at these radii is not viable for at least four reasons: (1) It is dynamically unstable when the dynamical time is $\ll 10^{6-7}$ yr ($R \ll 100$ pc), and cannot “support” a quasi-steady disk (Torrey et al. 2017). In brief, if one forms slightly “too many” massive stars (or they begin to blow away or exhaust or accrete even a small fraction of the disk gas so the disk gas mass decreases), the stars do not “turn off” until after their main-sequence lifetimes complete and they all finish exploding, so the feedback injection rate actually increases for this timescale (much longer than the dynamical time) and the blowout runs away. (2) As many studies have shown (Fall et al. 2010; Grudić et al. 2018, 2019, 2020; Ma et al. 2020; Hopkins et al. 2022, and references therein), above a critical acceleration scale $|\mathbf{a}| \sim G M_{\text{bh}}/R^2 \sim 10^{-7}$ cm s $^{-2}$ ($R \lesssim 40 m_7^{1/2}$ pc), stellar feedback from standard stellar populations/evolution tracks cannot inject sufficient momentum to “hold up” the disk without the mass of stars greatly exceeding the total gas mass, thus star formation greatly exceeding accretion rates and depleting the disk (preventing accretion). (3) Even if we ignore (1) and (2), a continuous feedback-regulated model predicts $Q \sim 1$ (Thompson et al. 2005; Ostriker & Shetty 2011; Cacciato et al. 2012; Krumholz et al. 2012; Hopkins et al. 2011, 2012; Orr et al. 2019, 2020, 2021), as discussed below for gravity, which Fig. 5 shows contradicts lower-limits from the maser kinematics. (4) The implied massive stellar density and

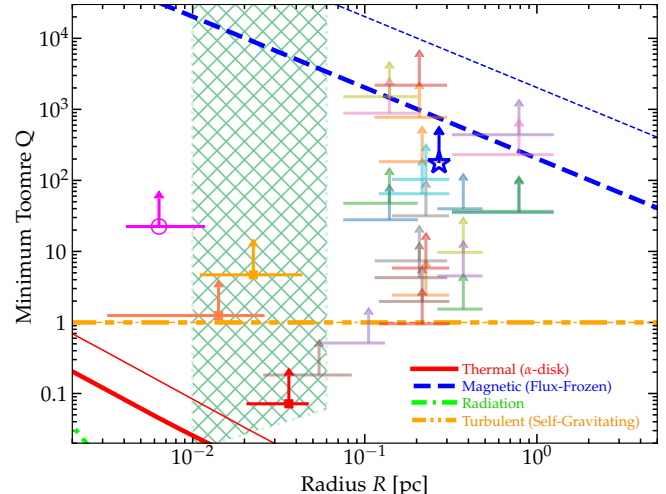


Fig. 5.— Observational limits and predictions (as Fig. 2) from different models for the minimum Toomre $Q(r)$ at a given radius r in the disk (§ 4.4.3), from kinematics alone (Eq. 28). We plot the “turbulent” line at $Q = Q_0 \sim 1$, the usual prediction for gravito-turbulent or self-regulating models. Below ~ 1 pc scales, maser data and some BLR constraints require a minimum $Q \gtrsim 20 - 1000$, much larger than gravitoturbulent predictions, and many orders of magnitude larger than predicted for thermal or radiation-pressure supported disks, but consistent with magnetically-supported disk models.

SNe rates in the disk (ignoring (1), (2), and (3), and imposing a steady-state model with the required parameters) would give stellar luminosities much larger than disk luminosities and stellar masses much larger than BH masses (i.e. $\Delta \gg 1$) in the outer disk, in addition to dense stellar “cusps” with orders-of-magnitude higher density than actually observed.⁶

4.4.3. Standard Gravito-Turbulent Disks Are Not Consistent with Observations

⁶ Specifically, to power the required turbulence would require, at any given time (assuming a standard IMF-integrated population; see Grudić et al. 2018; Shi et al. 2023, and using the scalings assuming we are inside the BHROI), a young (zero-age main sequence) stellar mass interior to r of $M_*^{\text{young}}/M_{\text{BH}} \gtrsim 10 m_8^{5/2} m_7^{-1/2} \alpha_{0.1}^{-1} \Delta_{0.01}^{-1} \gtrsim 110 m_7^{3/4} m^{1/2} \Delta_{0.01}^{1/2} r_{0.1}^{5/4} \alpha_{0.1}^{-1/2}$ (the latter using the minimum gas mass of the disk from § 2 to estimate n_8), i.e. $\Delta \gg 1$, and a stellar luminosity $L_* \gtrsim 100 L_{\text{BH}} n_8 r_{\text{pc}}^{5/2} m_7^{-1} \alpha_{0.1}^{-1} \Delta_{0.01}^{-1}$. The former exceeds unity meaning there is no self-consistent $\Delta \ll 1$ (close-to-Keplerian) solution, nor is there a solution which features stellar luminosity interior to the BHROI less than AGN/disk luminosity. Integrating over the accretion history of the BH (using $\int \dot{M} dt = M_{\text{BH}}$ by definition), this would imply a relic star cluster mass around the BH of at least $M_*^{\text{old}}/M_{\text{BH}} \gtrsim 30 n_8 r_{0.1}^{5/2} m_7^{-1/2} \alpha_{0.1}^{-1} \Delta_{0.01}^{-1}$, or $\Delta_{0.01} \gtrsim 50 n_8^{1/2} \alpha_{0.1}^{1/2} r_{0.1}^{5/4} m_7^{1/4}$, or stellar relic cusp surface density $\Sigma_* \gtrsim 10^{10} M_{\odot} \text{ pc}^{-2} m_7^{1/2} n_8 r_{0.1}^{1/2} \alpha_{0.1}^{-1} \Delta_{0.01}^{-1}$ which is five orders-of-magnitude larger than the maximum observed $\Sigma_* \lesssim 10^5 M_{\odot} \text{ pc}^{-2}$ in any circum-BH stellar cusp at these radii in the local Universe (Lauer et al. 2007; Côté et al. 2007; Kormendy et al. 2009; Hopkins et al. 2009a, 2010; Grudić et al. 2019).

So this leaves gravitational energy as the only remaining power source for a turbulent disk, if we do *not* allow for something like a magnetically-dominated disk. This would be a “gravitoturbulent” or “self-gravitating” disk. The problem is that the most robust and universal prediction of such models is that if the disk is “held up” and accretion powered by Reynolds stresses from gravity-driven turbulence (*without* another form of pressure comparable to or larger than the turbulence) then the disk must self-regulate at a turbulent Toomre Q parameter near unity (see references above and Paczynski 1978; Gammie 2001; Kim & Ostriker 2001; Sisko & Goodman 2003; Thompson et al. 2005; Riols & Latter 2016; Forgan et al. 2017; Deng et al. 2020). In other words:

$$Q_{\text{turb}}^{\text{pred}} \sim \frac{v_{\text{turb}}^{\text{pred}} \Omega}{\pi G \Sigma_{\text{gas}}^{\text{pred}}} = \frac{\Omega^2}{2\pi G \rho^{\text{pred}}} = Q_0 \sim 1 \quad (26)$$

Physically, if $Q \gg 1$, then the disk self-gravity is negligible, and it will simply sit in a stable Keplerian orbit without powering any turbulence or accretion, until some cooling or other dissipation or energy transfer or new accretion reduces Q to order-unity (while if $Q \ll 1$, these modes excite strong turbulence to bring Q back to ~ 1). But Eq. 26 immediately predicts a gas density

$$n_{\text{turb}}^{\text{pred}} \sim 10^{11} Q_0^{-1} \text{ cm}^{-3} m_7 r_{0.1}^{-3} \sim 10^{17} Q_0^{-1} \text{ cm}^{-3} m_7 r_{\text{ld}}^{-3}, \quad (27)$$

much higher than observed in the inner maser or broad line regions unless $Q_0 \gg 1$.⁷ More plainly, from Eqs. 10 and 26, we see that a given measurement or upper limit to Δ implies a corresponding *lower* limit to Q in the disk:

$$Q \gtrsim 20 \frac{r_{0.1}^{3/4} \dot{m}^{1/2}}{m_7^{1/4} \alpha_{0.1}^{1/2} \Delta_{0.01}^{3/2}}, \quad (28)$$

which ranges from $\sim 10 - 1000$ over the range of observations we consider at large radii, as shown in Fig. 5.

Related, let us now specifically consider the self-consistent predictions for such models – i.e. imposing not just $Q_0 \sim \text{constant}$, but $\dot{M} \sim \text{constant}$ with the only available stress, Reynolds stress $\sim \rho v_{\text{t}}^2$ driving accretion. This predicts $v_{\text{turb}} \sim (3 Q_0 G \dot{M}_{\text{BH}}/2)^{1/3}$ and

$$\begin{aligned} \frac{V_{c, \text{self}}^{\text{turb}}}{v_K} &\sim 0.3 \dot{m}^{1/6} m_7^{-1/6} Q_0^{-1/3} r_{0.1}^{1/4} \\ \frac{M_{\text{disk}}^{\text{turb}}}{M_{\text{BH}}} &\sim 0.1 \dot{m}^{1/3} r_{0.1}^{1/2} m_7^{-1/6} Q_0^{-2/3} \quad (29) \\ \frac{H_{\text{turb}}^{\text{pred}}}{R} &\sim 0.016 \frac{Q_0^{1/3} r_{0.1}^{1/2}}{m_7^{1/6}}, \quad (30) \end{aligned}$$

a much larger deviation from Keplerian rotation, and much thinner H/R , than allowed by maser observations (Eqs. 7-9) for $Q_0 \sim 1$. So the densities, disk masses, and scale-heights observed in maser data require that these models must self-regulate to $Q_0 \gtrsim 100$ (not $Q_0 \sim 1$) to be consistent with

⁷ And this is actually a *lower* limit to $n_{\text{turb}}^{\text{pred}}$, as we assumed isotropic turbulence, while a more careful derivation should multiply it by a factor of $\sim \delta v_R^{\text{turb}} / \delta v_z^{\text{turb}}$, the radial-to-vertical turbulent velocity dispersion ratio, which is typically $\gg 1$ in gravito-turbulence (because the salient gravitational modes only drive in-plane motions $\delta v_{R, \phi}^{\text{turb}}$; Hopkins et al. 2012, 2013, 2024b; Orr et al. 2018, 2019; Su et al. 2017).

observations at radii $\sim 0.1 - 1$ pc. Similarly, for the direct estimate in Circinus from Izumi et al. (2023) of $M_{\text{disk}}^{\text{Circ}} \sim 3500 - 6100 M_{\odot}$ at $r < 0.27$ pc, we have $M_{\text{disk}}^{\text{turb}} \sim 2 \times 10^5 M_{\odot} Q_0^{-2/3}$ predicted, requiring $Q_0 \sim 220 - 500$ at these radii to fit the observations.⁸

Even the systems which have claims for apparent self-gravitating disks (NGC 1068 and 3079) do not appear to fit the self-consistent gravito-turbulent models. Consider NGC 3079: if we take the implied disk properties from Kondratko et al. (2005) at face value (interpreting the deviations from Keplerian rotation as indicating the disk mass), then fitting the apparently observed disk mass with Eq. 29 would require $Q_0 \sim 0.04$,⁹ (similar to the estimates of Q_0 from the gas densities in Kondratko et al. (2005), using Eq. 26, which require $Q_0 \sim 0.01$). But at the same time, the scale-height constraints in Kondratko et al. (2005) – who note any such disk model must be very thick ($H/R \sim 0.15 - 1$) to fit their data – require (Eq. 30) $Q_0 \sim 100 - 2000$. These disagree by 4 – 5 orders of magnitude, indicating that the data cannot be fit by any constant- Q_0 turbulence-only model, and on top of this either value of Q_0 is orders-of-magnitude different from the prediction of gravito-turbulent or marginally self-gravitating disk models. The same problem appears in NGC 1068, with the disk-mass interpretation of Lodato & Bertin (2003) requiring $Q_0 \sim 0.03$, while scale-height constraints from Gallimore & Impellizzeri (2023) require $Q_0 \gtrsim 100$.

On the other hand, in a scenario like the magnetically-dominated disks from § 4.2.1, trans-Alfvénic, supersonic turbulence with velocities similar to Eq. 25 is not a problem with respect to these observations, as we have shown.

4.4.4. Magnetic Field Strengths in Turbulence-Dominated Disks

Briefly, although the turbulence-dominated scenario assumes negligible magnetic pressure, in practice if we had a supersonic, super-Alfvénic turbulent disk, we would expect to amplify the magnetic fields to $\sim 10 - 50\%$ of equipartition with turbulence (Federrath et al. 2014; Su et al. 2018; Guszejnov et al. 2020; Martin-Alvarez et al. 2022, and references therein). If we take the “self-consistent” turbulent models above and just treat this as a passive magnetic field, this predicts an in-plane typical magnetic field strength (assuming isotropic motions as the lower-limit to the in-plane component):

$$B_{\phi}^{\text{turb, pred}} \gtrsim \frac{2.2}{\sqrt{3}} G \left(\frac{E_B}{E_{\text{turb}}} \right)^{1/2} \frac{m_7^{5/6} \dot{m}^{1/3}}{Q_0^{1/6} r_{0.1}^{3/2}} \quad (31)$$

Just like with thermal-pressure dominated disks in § 4.1.3, we see in Fig. 4 the surprising result that (for plausible equipartition saturation strengths and $Q_0 \sim 1$) this would predict *larger* magnetic fields compared to the magnetically-dominated disks in § 4.2.3 (Eq. 21)! The reason is the same: the model predicts (for $Q_0 \sim 1$) much thinner, higher-density disks compared to the magnetically-dominated case, so to have trans-Alfvénic turbulence, the absolute value of $|B_{\parallel}|$ (in Gauss) must be correspondingly larger.

⁸ The scalings here and in § 4.4.4 assume $Q_0 \gtrsim 1$ which gives $M_{\text{disk}} < M_{\text{BH}}$ at the radii of interest. For $Q_0 \ll 1$, where at large radii $M_{\text{disk}} \gg M_{\text{BH}}$, these scalings are modified to $M_{\text{disk}}^{\text{turb}} = 4 \cdot 3^{2/3} \dot{M} R (G \dot{M})^{-1/3} Q_0^{-4/3} \sim 0.002 \dot{m}^{2/3} r_{0.1} m_7^{-1/3} Q_0^{-4/3}$, $n_{\text{turb}} \sim 2 \times 10^8 \text{ cm}^{-3} (m_7 \dot{m})^{2/3} r_{0.1}^{-2} Q_0^{-7/3}$, $H^{\text{turb}}/R \sim 0.33 Q_0$, $B_{\phi}^{\text{turb}} \sim 0.06 Q_0^{-5/6} (E_B/E_{\text{turb}})^{1/2} (m_7 \dot{m})^{2/3} r_{0.1}^{-1}$.

⁹ When $M_{\text{disk}}^{\text{turb}} \gtrsim M_{\text{BH}}$, Eq. 29 is modified to $M_{\text{disk}}^{\text{turb}} = 4 \cdot 3^{2/3} \dot{M} R (G \dot{M})^{-1/3} Q_0^{-4/3}$, but this requires $Q_0 \lesssim 0.008 \dot{m}^{1/2} r_{0.1}^{3/4} m_7^{1/4}$.

4.5. Cosmic Ray, Neutrino, or Degeneracy-Pressure Dominated Disks

For completeness, consider some other sources of pressure which are already widely-agreed to be ruled out for AGN accretion disks but can support accretion disks in other astrophysical systems: cosmic rays (CRs), neutrinos, and degeneracy pressure. The latter (neutrinos and degeneracy pressure) are immediately ruled out by any $\Delta \ll 10^{10}$ or so, let alone $\ll 1$, because the densities required for degeneracy pressure and/or non-negligible neutrino opacity are so many orders of magnitude larger than any which are permitted by dynamical constraints here (and the emission would be wildly different as well). The case of CRs is slightly less obvious, and they can be in equipartition with other pressures in Solar-neighborhood ISM disks (Webber 1998; Draine 2011; Amato & Blasi 2018). In a CR-pressure dominated disk, $P_{\text{tot}} \sim (1/3) u_{\text{cr}}$ in terms of the total energy density of CRs u_{cr} , dominated by $\sim 1-10$ GeV protons. First note however that there are *no* self-consistent solutions for a CR pressure-supported AGN accretion disk (this is why, of course, this is not usually discussed in this literature). If one equates the energy change from gravity or stresses with some $\Pi \leq P_{\text{cr}}$ to the CR loss rate, then the hadronic loss rate ($dE/dtd\text{Vol} \approx 3 \times 10^9 \text{ s}^{-1} (\rho/\text{g cm}^{-3}) P_{\text{cr}}$) at any reasonable density would be vastly too large to be replenished (there is no steady-state solution except at extremely low densities), but at low densities where these would balance the CR loss time becomes dominated by diffusive escape with timescale $\sim H^2/\kappa$ (for a diffusion coefficient κ). But that, in turn, gives a solution for H which is $\ll a$ at $r \sim \text{pc}$ (i.e. vastly too thin) and is always (for *any* κ allowed in this regime) orders of magnitude smaller than the CR scattering/deflection length ($\sim 3\kappa/c$), so the CRs could not “hold up” the disk. But even if we ignored all of these arguments and simply used our lower limit to Π/ρ , we would require a CR energy density $u_{\text{cr}} \sim 3 \times 10^9 \text{ eV cm}^{-3} \dot{m} n_8 m_7^{1/2} r_{0.1}^{1/2} \Delta_{0.01}^{-1}$, which is enormous compared to any reasonable estimates in galactic nuclei (Krumholz et al. 2023), and would imply an instantaneous γ -ray luminosity (using the hadronic scalings from Chan et al. 2019) at large radii of $L_\gamma \gtrsim 10^{46} \text{ erg s}^{-1} \dot{m}^{3/2} n_8^2 m_7^{1/4} \alpha^{-1/2} \Delta_{0.01}^{-3/2} r_{\text{pc}}^{17/4}$, far in excess of that observed. So we can safely rule out this class of models (as anticipated).

4.6. External Potential (Stellar/ISM) Zone

At large enough radii from the SMBH (around the BH radius of influence $[\text{BHROI}] \sim GM_{\text{BH}}/\sigma_*^2$ where σ_* is the stellar nuclear velocity dispersion), stars will begin to dominate the matter density and total enclosed mass at those radii from the SMBH. The assumptions in § 2 then no longer hold: of course, if the mass of stars becomes comparable to the BH itself, then V_c becomes non-Keplerian and $\Omega = V_c/R$ includes the contribution from stars – i.e. $\Delta \gg 1$. But more importantly, even if we somehow had $V_c \approx v_K$, if stars dominate the *local* density ($M_{\text{gas}}(< R) \lesssim M_*(< R) \ll M_{\text{BH}}$), then the stress driving accretion does not have to be an *internal* stress in the gas. In other words, if we write $\dot{M} = 3\pi v_{\text{v, eff}} \Sigma_{\text{gas}}$ with $v_{\text{v, eff}} \equiv \Pi_{\text{eff}}/(\rho\Omega)$, then we can have $\Pi_{\text{eff}} \rightarrow \Pi_{\text{ext}} \gg P_{\text{tot, gas}}$ in principle, where Π_{eff} represents an “external stress” from stars acting on gas. Indeed, in practice, in gas+stellar disks on ISM scales (where $M_* \gg M_{\text{gas}}$), $\Pi_{\text{ext}} \sim \eta_{\text{ext}} \rho V_c^2$ (with $\eta_{\text{ext}} \sim 0.01-1$; see Hopkins & Quataert 2010b, 2011b; Anglés-Alcázar et al. 2021) is generally the dominant stress, coming primarily from two sources: (1) direct feedback effects (e.g.

work done by expanding stellar winds or SNe on ambient gas), and (2) gravitational torques, i.e. non-axisymmetric torques from stars driving shocks and dissipation in the gas (Barnes & Hernquist 1996; Hopkins et al. 2009b, 2016, 2024a; Hopkins & Quataert 2010b; Cacciato et al. 2012; Querejeta et al. 2016; Prieto & Escala 2016; Prieto et al. 2017; Anglés-Alcázar et al. 2017, 2021; Williamson et al. 2022; Izquierdo-Villalba et al. 2023). One then obtains $\dot{M} \sim \eta_{\text{ext}} \dot{M}_{\text{gas}}(< R) \Omega$, so $M_{\text{gas}}/M_{\text{BH}} \sim \dot{m}/(\eta \Omega)$ or $\sim 0.001 \eta_{\text{ext}}^{-1} \dot{m} m_7^{1/4}$ at the BHROI. This then allows for efficient fueling of the SMBH even with a small disk *gas* mass at these radii (Hopkins & Quataert 2010b, 2011b). More importantly, for our purposes, it means that once the local density of stars becomes comparable to the density of gas and $\Delta \gtrsim 1$ (the behavior at/outside the BHROI), the system becomes “ISM like” rather than “accretion disk like” and the kinematic constraints above no longer translate to the same constraints regarding the nature of the accretion disk.

5. CONCLUSIONS

Kinematics of masers and the broad-line region strongly constrain the allowed masses and mass profiles of the outer accretion disk around accreting supermassive black holes. For any self-consistent accretion disk model (where the stresses driving accretion cannot exceed the total stress/pressure in the disk), we show that this translates to constraints on the physics of what dominates the pressure in the accretion disk, and rule out many models immediately, regardless of free parameters in the models.

We specifically show that *these constraints immediately rule out standard thermal-pressure dominated (“ α ”) disks akin to those in SS73*. Any self-consistent thermal pressure-dominated disk would have a mass larger than the SMBH and a steeply-rising rotation curve, clearly ruled out by the data. Even if we arbitrarily fit the temperature and α parameter of the disk as a function of radius so as to provide any desired pressure profile, we show this would predict disk temperatures so hot that (1) maser and BLR emission would be impossible and the spectrum of the QSO would be completely incorrect, and (2) the thermal emission would more than ten orders of magnitude larger than observed. The predicted gas densities, optical depths, and many other properties are also inconsistent with the fact that we see maser and BLR emission at these radii. We similarly immediately rule out any disk which is dominated by radiation or cosmic ray pressure at these radii.

Magnetic-pressure dominated disks, specifically recently-proposed models of “flux-frozen” hyper-magnetized ($\beta \ll 1$) disks, on the other hand, are consistent with the present observations. The predicted gas densities and temperatures from such theoretical disk models are also in agreement with those needed for the BLR and maser emission.

It is plausible that turbulence could provide an order-unity fraction of the total pressure (unlike thermal or radiation pressure). However, models where turbulence “alone” provides the pressure (without e.g. strong magnetic fields) are strongly constrained: we can immediately rule out models where such turbulence is powered by stellar feedback or by gravitational instabilities (“gravito-turbulent” or “marginally self-gravitating” disks). While there is sufficient energy in gravity to power turbulence, in the absence of other appreciable pressures like magnetic pressure, we show that gravito-turbulent models would have to self-regulate at more like a turbulent Toomre Q parameter of $\gtrsim 100$ (as opposed to the canonical ~ 1) in the outer disk, to be consistent with the observations.

We also show that, counter-intuitively, the self-consistent models for magnetically-dominated disks predict *weaker* absolute magnetic field strengths than either (a) thermal-pressure dominated α -disk models where the magnetic fields are provided by the MRI or the α arises from any Maxwell stress larger than or comparable to the Reynolds stress, or (b) gravitoturbulent disks with super-sonic and super-Alfvénic turbulence with Toomre $Q \sim 1$ driven by gravitational instabilities providing the Reynolds stress (assuming standard super-Alfvénic turbulent saturation). This is because even though the magnetic fields are *relatively* more important in the magnetically-dominated disks, the *absolute* pressures required in the disk to supply the observed accretion rates are orders-of-magnitude lower. The thermal-pressure-dominated disks, in particular, appear to also be independently ruled out by existing observations of maser Zeeman splitting. Surprisingly, *stronger upper limits on magnetic fields favor more magnetically-dominated disks*.

Together, this appears to strongly favor the hypothesis that the *outer* disks around AGN (at radii $R \gtrsim 1000 R_G \sim 0.01$ pc to the BH radius of influence at \gtrsim pc) are in a magnetically-dominated, flux-frozen state. Improved kinematic constraints can strengthen this conclusion and apply it to an even larger range of AGN. At much larger radii (\gg pc), while of course it is still interesting to understand what dominates the pressure and thermal structure of the ISM, it is not meaningful to speak of “accretion disk” solutions, since the gas is fully in the star-forming ISM and does not “feel” the BH potential and the dominant stresses can be extrinsic to the gas (from e.g. stellar bars or spiral arms or supernovae or colliding winds).

At much smaller radii $\sim 1 - 100 R_G$, where most of the thermal emission from the AGN originates, SS73-like models are most often assumed. While some of the BLR constraints we consider reach radii as small as ~ 0.003 pc (a few light-days) and $R \sim 200 - 300 R_G$ (around more massive BHs), unfortunately even much more precise measurements of rotation curves alone will not distinguish between models ef-

fectively at much smaller radii. This is because, although models here predict very different accretion disk masses even as $R \rightarrow 0$, they all predict the disk mass is very small compared to the BH mass ($M_{\text{disk}} \ll M_{\text{BH}}$) at such small radii, so gravitational deviations from Keplerian motion become tiny and basically undetectable. However, the different models also predict orders-of-magnitude different midplane densities, optical depths, accretion timescales, and scale heights H for the disks: these could potentially be measured directly (rather than inferred indirectly through kinematics as we do here), with sufficiently high-resolution data, and would provide powerful model discriminants.

One important question is whether the systems studied here (for which interesting kinematic constraints are available) actually form a representative subsample. For example, in principle one might argue that standard α -disks, apparently ruled out here, are prevalent in other AGN at large radii but somehow cannot produce masers, so only magnetically-dominated disks would be represented in those samples. However this seems unlikely. First, we obtain qualitatively consistent constraints from a wide variety of methods studying different types of objects: maser kinematics, resolved interferometry of nearby (lower-luminosity) BLRs, microlensing, BLR reverberation mapping, and direct imaging of neutral gas disks. It seems implausible that all of these suffer from the same biases. Second, there is no evidence that any of the sub-populations for which these constraints are measured are highly biased from the general population of quasars in other properties that might be indicative of the type of accretion disk, like their thermal continuum SED shapes. Still, this provides further motivation to expand all of these samples to more diverse AGN populations.

Support for PFH was provided by a Simons Investigator Grant.

REFERENCES

Abramowicz M. A., Fragile P. C., 2013, *Living Reviews in Relativity*, **16**, 1

Abramowicz M. A., Czerny B., Lasota J. P., Szuszkiewicz E., 1988, *ApJ*, **332**, 646

Adams F. C., Ruden S. P., Shu F. H., 1989, *ApJ*, **347**, 959

Amato E., Blasi P., 2018, *Advances in Space Research*, **62**, 2731

Anglés-Alcázar D., Davé R., Faucher-Giguère C.-A., Özel F., Hopkins P. F., 2017, *MNRAS*, **464**, 2840

Anglés-Alcázar D., et al., 2021, *ApJ*, **917**, 53

Bacon R., Emsellem E., Combes F., Copin Y., Monnet G., Martin P., 2001, *A&A*, **371**, 409

Balbus S. A., 2003, *ARA&A*, **41**, 555

Balbus S. A., Hawley J. F., 1998, *Reviews of Modern Physics*, **70**, 1

Barnes J. E., Hernquist L., 1996, *ApJ*, **471**, 115

Bentz M. C., et al., 2009, *ApJ*, **705**, 199

Braatz J. A., Henkel C., Greenhill L. J., Moran J. M., Wilson A. S., 2004, *ApJ*, **617**, L29

Braibant L., Hutsemékers D., Sluse D., Goosmann R., 2017, *A&A*, **607**, A32

Cacciato M., Dekel A., Genel S., 2012, *MNRAS*, **421**, 818

Cackett E. M., Bentz M. C., Kara E., 2021, *iScience*, **24**, 102557

Chan T. K., Kereš D., Hopkins P. F., Quataert E., Su K. Y., Hayward C. C., Faucher-Giguère C. A., 2019, *MNRAS*, **488**, 3716

Côté P., et al., 2007, *ApJ*, **671**, 1456

Das U., Begelman M. C., Lesur G., 2018, *MNRAS*, **473**, 2791

Davis S. W., Tchekhovskoy A., 2020, *ARA&A*, **58**, 407

Deng H., Mayer L., Latter H., 2020, *ApJ*, **891**, 154

Dietrich M., et al., 2012, *ApJ*, **757**, 53

Draine B. T., 2011, *Physics of the Interstellar and Intergalactic Medium*. Princeton University Press, Princeton, NJ, USA

Fall S. M., Krumholz M. R., Matzner C. D., 2010, *ApJ*, **710**, L142

Federrath C., Schober J., Bovino S., Schleicher D. R. G., 2014, *ApJ*, **797**, L19

Fian C., Jiménez-Vicente J., Mediavilla E., Muñoz J. A., Chelouche D., Kaspi S., Forés-Toribio R., 2024, *ApJ*, **972**, L7

Forgan D., Price D. J., Bonnell I., 2017, *MNRAS*, **466**, 3406

Frank J., King A., Raine D. J., 2002, *Accretion Power in Astrophysics*: Third Edition, isbn 0521620538 edn. Cambridge, UK: Cambridge University Press, Cambridge, UK

GRAVITY Collaboration et al., 2020, *A&A*, **643**, A154

GRAVITY Collaboration et al., 2021, *A&A*, **648**, A117

GRAVITY Collaboration et al., 2024, *arXiv e-prints*, p. arXiv:2401.07676

Gaburov E., Johansen A., Levin Y., 2012, *ApJ*, **758**, 103

Gallimore J. F., Impellizzeri C. M. V., 2023, *ApJ*, **951**, 109

Gammie C. F., 2001, *ApJ*, **553**, 174

Gao F., et al., 2017, *ApJ*, **834**, 52

Gravity Collaboration et al., 2018, *Nature*, **563**, 657

Greenhill L. J., Jiang D. R., Moran J. M., Reid M. J., Lo K. Y., Claussen M. J., 1995, *ApJ*, **440**, 619

Grudić M. Y., Hopkins P. F., Faucher-Giguère C.-A., Quataert E., Murray N., Kereš D., 2018, *MNRAS*, **475**, 3511

Grudić M. Y., Hopkins P. F., Quataert E., Murray N., 2019, *MNRAS*, **483**, 5548

Grudić M. Y., Boylan-Kolchin M., Faucher-Giguère C.-A., Hopkins P. F., 2020, *MNRAS*, **496**, L127

Guo M., Stone J. M., Quataert E., Kim C.-G., 2024, *arXiv e-prints*, p. arXiv:2405.11711

Guo M., Quataert E., Squire J., Hopkins P. F., Stone J. M., 2025, *arXiv e-prints*, p. arXiv:2505.12671

Guszejnov D., Grudić M. Y., Offner S. S. R., Boylan-Kolchin M., Faucher-Giguère C.-A., Wetzel A., Benincasa S. M., Loebman S., 2020, *MNRAS*, **492**, 488

Heinemann T., Papaloizou J. C. B., 2009, *MNRAS*, **397**, 52

Henkel C., Peck A. B., Tarchi A., Nagar N. M., Braatz J. A., Castangia P., Moscadelli L., 2005, *A&A*, **436**, 75

Herrnstein J. R., Moran J. M., Greenhill L. J., Trotter A. S., 2005, *ApJ*, **629**, 719

Hickox R. C., Alexander D. M., 2018, *ARA&A*, **56**, 625

Hopkins P. F., 2010, arXiv e-prints, arXiv:1009.4702 [astro-ph],

Hopkins P. F., 2025, *The Open Journal of Astrophysics*, **8**, 56

Hopkins P. F., Quataert E., 2010a, *MNRAS*, **405**, L41

Hopkins P. F., Quataert E., 2010b, *MNRAS*, **407**, 1529

Hopkins P. F., Quataert E., 2011a, *MNRAS*, **411**, L61

Hopkins P. F., Quataert E., 2011b, *MNRAS*, **415**, 1027

Hopkins P. F., Cox T. J., Dutta S. N., Hernquist L., Kormendy J., Lauer T. R., 2009a, *ApJS*, **181**, 135

Hopkins P. F., Cox T. J., Younger J. D., Hernquist L., 2009b, *ApJ*, **691**, 1168

Hopkins P. F., Murray N., Quataert E., Thompson T. A., 2010, *MNRAS*, **401**, L19

Hopkins P. F., Quataert E., Murray N., 2011, *MNRAS*, **417**, 950

Hopkins P. F., Quataert E., Murray N., 2012, *MNRAS*, **421**, 3488

Hopkins P. F., Kereš D., Murray N., 2013, *MNRAS*, **432**, 2639

Hopkins P. F., Torrey P., Faucher-Giguère C.-A., Quataert E., Murray N., 2016, *MNRAS*, **458**, 816

Hopkins P. F., Wellons S., Anglés-Alcázar D., Faucher-Giguère C.-A., Grudić M. Y., 2022, *MNRAS*, **510**, 630

Hopkins P. F., et al., 2024a, *The Open Journal of Astrophysics*, **7**, 18

Hopkins P. F., et al., 2024b, *The Open Journal of Astrophysics*, **7**, 19

Hopkins P. F., et al., 2024c, *The Open Journal of Astrophysics*, **7**, 20

Hopkins P. F., Grudic M. Y., Kremer K., Offner S. S. R., Guszejnov D., Rosen A. L., 2024d, *The Open Journal of Astrophysics*, **7**, 71

Hopkins P. F., et al., 2025, *The Open Journal of Astrophysics*, **8**, 48

Hutsemékers D., Sluse D., Savić Đ., 2024a, *A&A*, **687**, A153

Hutsemékers D., Sluse D., Savić Đ., 2024b, *A&A*, **691**, A292

Ito R., Miyamoto Y., Nakai N., Yamauchi A., Terashima Y., 2025, arXiv e-prints, p. [arXiv:2510.10354](https://arxiv.org/abs/2510.10354)

Izquierdo-Villalba D., Lupi A., Regan J., Bonetti M., Franchini A., 2023, arXiv e-prints, p. [arXiv:2311.03152](https://arxiv.org/abs/2311.03152)

Izumi T., et al., 2023, *Science*, **382**, 554

Jacobs V., Sellwood J. A., 2001, *ApJ*, **555**, L25

Jiang Y.-F., Stone J. M., Davis S. W., 2019, *ApJ*, **880**, 67

Kaaz N., Liska M. T. P., Jacquemin-Ide J., Andelman Z. L., Musoke G., Tchekhovskoy A., Porth O., 2023, *ApJ*, **955**, 72

Kaaz N., Liska M., Tchekhovskoy A., Hopkins P. F., Jacquemin-Ide J., 2025, *ApJ*, **979**, 248

Kaspi S., Smith P. S., Netzer H., Maoz D., Jannuzi B. T., Giveon U., 2000, *ApJ*, **533**, 631

Kim W.-T., Ostriker E. C., 2001, *ApJ*, **559**, 70

Kollatschny W., Bischoff K., Robinson E. L., Welsh W. F., Hill G. J., 2001, *A&A*, **379**, 125

Kondratko P. T., Greenhill L. J., Moran J. M., 2005, *ApJ*, **618**, 618

Kondratko P. T., et al., 2006a, *ApJ*, **638**, 100

Kondratko P. T., Greenhill L. J., Moran J. M., 2006b, *ApJ*, **652**, 136

Kondratko P. T., Greenhill L. J., Moran J. M., 2008, *ApJ*, **678**, 87

Kormendy J., Fisher D. B., Cornell M. E., Bender R., 2009, *ApJS*, **182**, 216

Krumholz M. R., Dekel A., McKee C. F., 2012, *ApJ*, **745**, 69

Krumholz M. R., Crocker R. M., Offner S. S. R., 2023, *MNRAS*, **520**, 5126

Kudoh Y., Wada K., Norman C., 2020, *ApJ*, **904**, 9

Kuo C. Y., et al., 2011, *ApJ*, **727**, 20

Kuo C. Y., Reid M. J., Braatz J. A., Gao F., Impellizzeri C. M. V., Chien W. T., 2018, *ApJ*, **859**, 172

Kuo C. Y., et al., 2020, *MNRAS*, **498**, 1609

Läsker R., Greene J. E., Seth A., van de Ven G., Braatz J. A., Henkel C., Lo K. Y., 2016, *ApJ*, **825**, 3

Lauer T. R., et al., 2007, *ApJ*, **664**, 226

Linzer N. B., Goulding A. D., Greene J. E., Hickox R. C., 2022, arXiv e-prints, p. [arXiv:2208.01669](https://arxiv.org/abs/2208.01669)

Lira P., et al., 2018, *ApJ*, **865**, 56

Lodato G., Bertin G., 2003, *A&A*, **398**, 517

Lonsdale C. J., Lonsdale C. J., Smith H. E., Diamond P. J., 2003, *ApJ*, **592**, 804

Lopez-Rodriguez E., et al., 2013, *MNRAS*, **431**, 2723

Lu K.-X., et al., 2021, *ApJ*, **918**, 50

Luo Y., Shlosman I., 2024, *ApJ*, **976**, 85

Ma X., et al., 2020, *MNRAS*, **493**, 4315

Maoz E., 1995, *ApJ*, **455**, L131

Martin-Alvarez S., Devriendt J., Slyz A., Sijacki D., Richardson M. L. A., Katz H., 2022, *MNRAS*, **513**, 3326

McCallum J. N., Ellingsen S. P., Lovell J. E. J., 2007, *MNRAS*, **376**, 549

Miyoshi M., Moran J., Herrnstein J., Greenhill L., Nakai N., Diamond P., Inoue M., 1995, *Nature*, **373**, 127

Modzak M., Moran J. M., Kondratko P. T., Greenhill L. J., 2005, *ApJ*, **626**, 104

Moran J., Greenhill L., Herrnstein J., Diamond P., Miyoshi M., Nakai N., Inoue M., 1995, *Proceedings of the National Academy of Science*, **92**, 11427

Murray N., Chiang J., Grossman S. A., Voit G. M., 1995, *ApJ*, **451**, 498

Novikov I. D., Thorne K. S., 1973, in *Black Holes (Les Astres Occlus)*. pp 343–450

Orr M. E., et al., 2018, *MNRAS*, **478**, 3653

Orr M. E., Hayward C. C., Hopkins P. F., 2019, *MNRAS*, **486**, 4724

Orr M. E., et al., 2020, *MNRAS*, **496**, 1620

Orr M. E., et al., 2021, *ApJ*, **908**, L31

Ostriker E. C., Shetty R., 2011, *ApJ*, **731**, 41

Paczynski B., 1978, *Acta Astron.*, **28**, 91

Paczynsky B., Wiita P. J., 1980, *A&A*, **88**, 23

Panessa F., Castangia P., Malizia A., Bassani L., Tarchi A., Bazzano A., Ubertini P., 2020, *A&A*, **641**, A162

Pesce D. W., Braatz J. A., Condon J. J., Gao F., Henkel C., Litzinger E., Lo K. Y., Reid M. J., 2015, *ApJ*, **810**, 65

Pessah M. E., Chan C.-K., Psaltis D., 2006, *MNRAS*, **372**, 183

Peterson B., 2006, *The Broad-Line Region in Active Galactic Nuclei*. Springer Berlin Heidelberg (Eds. Alloin, Danielle and Johnson, Rachel and Lira, Paulina), Berlin, Heidelberg, pp 77–100, doi:10.1007/3-540-34621-X_3, https://doi.org/10.1007/3-540-34621-X_3

Peterson B. M., Wandel A., 1999, *ApJ*, **521**, L95

Peterson B. M., et al., 2004, *ApJ*, **613**, 682

Piotrovich M., Buliga S., Natsvlishvili T., 2021, *Universe*, **7**, 202

Prieto J., Escala A., 2016, *MNRAS*, **460**, 4018

Prieto J., Escala A., Volonteri M., Dubois Y., 2017, *ApJ*, **836**, 216

Querejeta M., et al., 2016, *A&A*, **588**, A33

Riols A., Latter H., 2016, *MNRAS*, **460**, 2223

Schmidt M., 1963, *Nature*, **197**, 1040

Shakura N. I., Sunyaev R. A., 1973, *A&A*, **24**, 337

Shi Y., Kremer K., Grudic M. Y., Gerling-Dunsmore H. J., Hopkins P. F., 2023, *MNRAS*, **518**, 3606

Shi Y., Kremer K., Hopkins P. F., 2024a, *A&A*, **691**, A24

Shi Y., Kremer K., Hopkins P. F., 2024b, *ApJ*, **969**, L31

Silant'ev N. A., Piotrovich M. Y., Gnedin Y. N., Natsvlishvili T. M., 2010, *Astronomy Letters*, **36**, 549

Sirk E., Goodman J., 2003, *MNRAS*, **341**, 501

Soltan A., 1982, *MNRAS*, **200**, 115

Squire J., Quataert E., Hopkins P. F., 2025, *The Open Journal of Astrophysics*, **8**, 39

Su K.-Y., Hopkins P. F., Hayward C. C., Faucher-Giguère C.-A., Kereš D., Ma X., Robles V. H., 2017, *MNRAS*, **471**, 144

Su K.-Y., Hayward C. C., Hopkins P. F., Quataert E., Faucher-Giguère C.-A., Kereš D., 2018, *MNRAS*, **473**, L111

Thompson T. A., Quataert E., Murray N., 2005, *ApJ*, **630**, 167

Torrey P., Hopkins P. F., Faucher-Giguère C.-A., Vogelsberger M., Quataert E., Kereš D., Murray N., 2017, *MNRAS*, **467**, 2301

Touma J. R., 2002, *MNRAS*, **333**, 583

Tremaine S., 2001, *AJ*, **121**, 1776

Vernardos G., et al., 2024, *Space Sci. Rev.*, **220**, 14

Vlemmings W. H. T., Bignall H. E., Diamond P. J., 2007, *ApJ*, **656**, 198

Wang H.-Y., Guo M., Most E. R., Hopkins P. F., Lalakos A., 2025, arXiv e-prints, p. [arXiv:2504.03874](https://arxiv.org/abs/2504.03874)

Webber W. R., 1998, *ApJ*, **506**, 329

Williamson D. J., Bösch L. H., Höning S. F., 2022, *MNRAS*, **510**, 5963

Yuan F., Narayan R., 2014, *ARA&A*, **52**, 529

Zu Y., Kochanek C. S., Peterson B. M., 2011, *ApJ*, **735**, 80

This paper was built using the Open Journal of Astrophysics \LaTeX template. The OJA is a journal which provides fast and easy peer review for new papers in the `astro-ph` section of the

arXiv, making the reviewing process simpler for authors and referees alike. Learn more at <http://astro.theoj.org>.